Accepted Manuscript

Novel 6-(piperazin-1-yl)phenanthridine amide and sulphonamide derivatives as potent *Mycobacterium tuberculosis* H37Rv inhibitors

Kalaga Mahalakshmi Naidu, Hunsur Nagendra Nagesh, Manjeet Singh, Dharmarajan Sriram, Perumal Yogeeswari, Kondapalli Venkata Gowri Chandra Sekhar

PII: S0223-5234(15)00033-1

DOI: 10.1016/j.ejmech.2015.01.013

Reference: EJMECH 7629

To appear in: *European Journal of Medicinal Chemistry*

Received Date: 30 September 2014

Revised Date: 22 November 2014

Accepted Date: 8 January 2015

Please cite this article as: K.M. Naidu, H.N. Nagesh, M. Singh, D. Sriram, P. Yogeeswari, K.V. Gowri Chandra Sekhar Novel 6-(piperazin-1-yl)phenanthridine amide and sulphonamide derivatives as potent *Mycobacterium tuberculosis* H37Rv inhibitors, *European Journal of Medicinal Chemistry* (2015), doi: 10.1016/j.ejmech.2015.01.013.

Novel 6-(piperazin-1-yl)phenanthridine amide and sulphonamide derivatives as potent *Mycobacterium tuberculosis* H37Rv inhibitors

Kalaga Mahalakshmi Naidu,[a] Hunsur Nagendra Nagesh,[a] Manjeet Singh,[b] Dharmarajan Sriram,[c] Perumal Yogeeswari,[c] Kondapalli Venkata Gowri Chandra Sekhar[a*]

[a]*Department of Chemistry, Birla Institute of Technology & Science-Pilani, Hyderabad campus, Jawahar Nagar, Shamirpet Mandal, Hyderabad-500 078, India.*

[b]*Department of Chemistry, Banaras Hindu University, Varanasi- 221 005, India.*

[c]*Department of Pharmacy, Birla Institute of Technology & Science-Pilani, Hyderabad campus, Jawahar Nagar, Shamirpet Mandal, Hyderabad-500 078, India.*

33 novel compounds are synthesized and evaluated for their anti-TB activity. Amongst these, 3 compounds exhibited excellent anti-TB activity with MIC 1.56 µg/mL and SI for these compounds was >46.

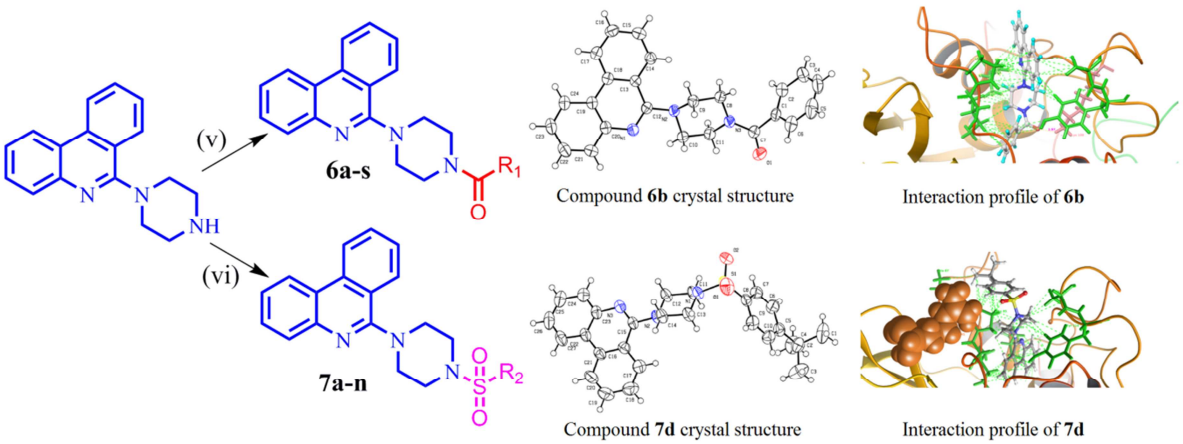

Novel 6-(piperazin-1-yl)phenanthridine amide and sulphonamide derivatives as potent *Mycobacterium tuberculosis* H37Rv inhibitors

Kalaga Mahalakshmi Naidu,[a] Hunsur Nagendra Nagesh,[a] Manjeet Singh,[b] Dharmarajan Sriram,[c] Perumal Yogeeswari,[c] Kondapalli Venkata Gowri Chandra Sekhar[a*]

[a]*Department of Chemistry, Birla Institute of Technology & Science-Pilani, Hyderabad campus, Jawahar Nagar, Shamirpet Mandal, Hyderabad-500 078, India.*
[b]*Department of Chemistry, Banaras Hindu University, Varanasi- 221 005, India.*
[c]*Department of Pharmacy, Birla Institute of Technology & Science-Pilani, Hyderabad campus, Jawahar Nagar, Shamirpet Mandal, Hyderabad-500 078, India.*

Abstract: A series of thirty three novel 6-(piperazin-1-yl)phenanthridine amide and sulphonamide analogues were synthesized, characterized and screened for their *in vitro* antimycobacterial activity against *Mycobacterium tuberculosis* (MTB) H37Rv strain. These compounds exhibited minimum inhibitory concentration (MIC) between 1.56 - ≥50 µg/mL. Out of these derivatives, few compounds **6l, 6r, 7b, 7f, 7g** and **7k** exhibited moderate activity (MIC = 6.25 µg/mL) and compounds **6b, 6e, 6k, 6n, 7h, 7i** and **7n** displayed good activity (MIC = 3.13 µg/mL), whereas compounds **6m, 6s** and **7d** exhibited excellent anti-tubercular activity (MIC = 1.56 µg/mL). In addition, MTT assay was accomplished on the active analogues of the series against mouse macrophage (RAW 264.7) cells to evaluate the toxicity profile of the newly synthesized compounds and selectivity index of the compounds was determined. Additionally, compounds **6b** and **7d** were docked to the ATPase domain of *Mycobacterium tuberculosis* GyrB protein to know the interaction profile and structures of compounds **6b** and **7d** were further substantiated through single crystal XRD.

Keywords: Phenanthridine; antimycobacterial activity; piperazine sulphonamide; *Mycobacterium tuberculosis*; single crystal XRD.

1. Introduction

* Corresponding author; Tel: +91-40-66303527; Fax: +91-40-66303998
E-mail address: kvgc@hyderabad.bits-pilani.ac.in; kvgcs@yahoo.com

Tuberculosis (TB) is a contagious disease caused by tubercular bacilli. In spite of several efforts by scientists across the world, this ancient scourge cannot be curtailed. It remains as one of the major public health concerns after the human immunodeficiency virus. Worldwide in 2013, 9 million people fell ill with TB, including 1.1 million cases among people living with HIV. 1.5 million died from TB, including 0.36 million who were HIV-positive. An estimated 0.48 million people developed multidrug-resistant TB (MDR-TB) and there were an estimated 0.21 million deaths from MDR-TB. Around 9.0 % of MDR-TB cases have extensively drug-resistant TB **(**XDR-TB). Around 100 countries have XDR-TB cases. More than 50 companies are involved in the development of new TB drugs. Since last four decades there are no new anti TB drugs except for Bedaquiline and Delamanid which became the first novel TB drugs approved. These two are used only for the treatment of pulmonary MDR-TB patients in serious or life-threatening conditions [1,2]. TB drug discovery and development has not progressed to the extent necessary to annihilate the illness completely. Hence, it is extremely essential to examine new compounds to cure against drug resistant forms of this mortal disease along with minimal side effects. Focus should also be on developing compounds which not only reduce the cost, but also the treatment period.

Phenanthridine derivatives are significant core moieties found in a variety of natural products, important class of alkaloids and other synthetic vital molecules with a wide range of biological activities and applications, including antibacterial [3,4], anticancer [5,6], antimalarial [7], anti-HIV [8], anti-HCV agents [9], antiplasmodial [10] and in particular as antitubercular agents [11-15]**.** Recently, Cappoen et al reported 1,2,3,4,8,9,10,11-Octahydrobenzo[*j*]phenanthridine-7,12-diones as new leads against *Mycobacterium tuberculosis* [11]. Our group also recently reported synthesis and evaluation of anti-tubercular activity of 6-(4-substitutedpiperazin-1-yl) phenanthridine analogues as anti-TB agents [12].

Lipophilicity of compounds plays an important role in the biological activities which they display. Attaching an alkyl/aryl amide and sulphonamides enhances the lipophilicity of compounds [16,17]. Consequently, alkyl/aryl amide and alkyl/aryl sulphonamide derivatives are known to exhibit wide range of pharmacological activities and physiochemical properties. Indeed, these alkyl/aryl amide and alkyl/aryl sulphonamide analogues display enhanced antibacterial and anti-TB activity [17-22].

In the quest for developing novel anti-TB agents we recently reported two compounds with sulphonamide moiety [13]. Interestingly out of the two compounds, one of them exhibited excellent anti-TB activity (MIC = 1.56 µg/mL) and this prompted us to explore further structure activity relationship (SAR) of the compounds and hence prepared this series of

compounds based on sulphonamides. Since carboxamides are analogous to sulphonamides, we also decided to synthesise various amide derivatives and study their SAR. Hence, we designed new (substituted)(4-(phenanthridin-6-yl)piperazin-1-yl)methanone and 6-(4-((4-substituted)sulfonyl)piperazin-1-yl)phenanthridine derivatives expecting increased biological activity to combat this fatal disease. Design strategy to achieve title compounds [11-15, 17-22] is depicted in **figure 1**.

2. Chemistry

In this report, we chalked out for the synthesis of 6-(4-substitutedpiperazin-1-yl) phenanthridine derivatives starting from 9-fluorenone as outlined in **Scheme 1**. We synthesized compound **5** according to our reported protocol with slight modification [12]. 9-fluorenone upon treatment with hydroxylamine hydrochloride and sodium acetate afforded *N*-hydroxy-9*H*-fluoren-9-imine **(2)**. Further heating **2** with polyphosphoric acid and phosphorus pentoxide gave phenanthridin-6(5*H*)-one **(3)**. 6-chlorophenanthridine (**4**) was synthesized by refluxing **3** with phosphorus oxychloride and *N*,*N*-dimethylaniline. Cardinal synthon 6-(piperazin-1-yl)phenanthridine (**5**) was prepared by irradiating a mixture of 6-chlorophenanthridine, anhydrous piperazine, triethylamine (TEA) and *N*,*N*-dimethylformamide (DMF) under microwave conditions.

Initially, we tried monitoring the reaction conditions with various bases and solvents as summarised in **Table 1**. We set off our investigation for the synthesis of **6b,** under various reaction conditions. As a model reaction, compound (**5**) was treated with various acids and amide coupling reagents were employed to get desired compound (entry 1-11). Initially, we employed TEA as base, 1-ethyl-3-(3-dimethylaminopropyl)carbodiimide (EDC.HCl) and 1-hydroxybenzotriazole (HOBt) as amide coupling reagents in the presence of dichloromethane (DCM) as solvent at 0 ^{o}C to rt. Resultant mixture was stirred for 8h to yield **6b** in about 58% (entry 1). Changing the solvent to DMF under similar reaction conditions yielded **6b** in about 52%. Alternatively, changed amide coupling reagents such as 1-[Bis(dimethylamino)methylene]-1H-1,2,3-triazolo[*4,5-b*]pyridinium 3-oxid hexafluoro phosphate (HATU), (Benzotriazol-1-yloxy)tris(dimethylamino)phosphonium hexafluorophosphate (BOP) and (Benzotriazol-1-yloxy)tripyrrolidinophosphonium hexafluorophosphate (PyBOP) and solvent as *N*,*N*-diisopropylethylamine (DIPEA) under similar condition yields are 38-42% (entry 3–5). Next we hope to improve the yields, 1-Propanephosphonic anhydride (T_3P) was employed to alleviate the yield (entry 6-11). Initially, the reaction was carried out with various bases and solvents (entry 6-7) to give the desired compound in moderate yield. The reaction was further optimised with TEA and DCM

at various intervals of time (entry 8-11), to give **6b** in good yield. Found entries 9-10 potently improved the yield and actuate reaction period 6-8 h and reputable technique. Having the optimised reaction conditions handy, a series of **19** compounds **6a-s** was synthesized in good yield, thus validating the scope of the present protocol.

Further, compound **5** was reacted with various sulfonyl chlorides, using TEA as base and DCM as solvent at 0 ºC to rt for 1-2 h to yield **7a-n** in good yields. All the title compounds were purified by column chromatography. Both analytical and spectral data (^{1}H NMR, ^{13}C NMR, FTIR, Elemental analysis and MS) of all the synthesized compounds were confirmed prior to their evaluation of antimycobacterial activity.

In general, nucleophilic aromatic substitution at 6-chlorophenanthridine was confirmed by FTIR analysis of key synthon **5** which showed the disappearance of IR absorption peak at ~754 cm^{-1} due to aromatic C-Cl stretching frequencies and further disappearance of weak band at ~3280 cm^{-1} in the IR spectra of 6-(piperazin-1-yl)phenanthridine **(5)** confirms the formation of title compounds (**6a-s** and **7a-n).** In general, ^{1}H NMR spectrum of final compounds displayed 8 aromatic protons of phenanthridine in the range δ 7.32 - 8.74 and 8 aliphatic piperazine (-CH_2-) protons were observed in the range δ 3.42 - 4.28. The spectral data of all the title compounds are provided in experimental section.

3. Results and discussion

3.1. Antimycobacterial activity

All the synthesized compounds were tested for their ability to inhibit the growth of MTB H37Rv strain by Microplate Alamar Blue Assay (MABA) with compound concentration ranging from 50 to 0.78 µg/mL. Isoniazid, Rifampicin and Pyrazinamide were used as the positive drug standards. The *in vitro* test results for title compounds tabulated in **Table 2** indicate that MIC ranges from 1.56 to ≥ 50 µg/mL. Compounds with MIC 1.56 – 12.5 µg/mL were further subjected to cytotoxicity studies. In these analogues, compounds **6m, 6s** and **7d** are found to be excellent promising candidates by inhibiting 99% growth of MTB H37Rv (ATCC 27294) strain at 1.56 µg/mL concentration.

Among the synthesized compounds, electronic effects of substituent play an important role in displaying anti-TB activity. 6-(piperazin-1-yl)phenanthridine (**5**) was inhibiting 99% growth of MTB H37Rv strain at 25 µg/mL [12]. Amongst, phenanthridine amides (**6a-s)** and phenanthridine sulphonamide **(7a-n)** derivatives MTB activity summary, SAR studies are described based on activity of compound **5**. Introduction of cyanoacetyl group (**6a**) at the 4th position of compound **5,** retained the anti-TB activity with MIC 25 µg/mL. Presence of amine an electron donating group (EDG) at either ortho (**6g**) or para (**6h**) position on phenyl ring

decreased the activity by ≥2 fold. Introduction of nitro group, an electron withdrawing group (EWG), at meta (**6e**) position on phenyl ring greatly enhanced anti-TB activity by 8 fold with MIC 3.13 µg/mL. On the other hand nitro group at di-meta (**6f**) and para (**6d**) position on phenyl ring, decreased activity by 1-2 folds. Presence of chloro an EWG at para (**6c**) position on phenyl ring improved anti-TB activity by 2 fold with MIC 12.5 µg/mL. Benzoyl group (**6b**) at 4th position of compound **5** significantly increased anti-TB activity by 8 folds with MIC 3.13 µg/mL; cinnamoyl group (**6j**) at 4th position of **5** increased activity by 2 folds with MIC 12.5 µg/mL and 2-(naphthalen-1-yl)acetyl group (**6i**) at 4th position of compound **5** critically decreased the anti-TB activity by >2 folds with MIC >50 µg/mL. To establish extensive SAR we also varied heterocyclic compounds such as five membered rings (furan and thiophene), six membered ring (pyridyls) and indole analogues. Furan-2-carbonyl group (**6o**) and thiophene-2-carbonyl group (**6p**) at 4th position of 6-(piperazin-1-yl)phenanthridine (**5**) retained and decreased anti-TB activity by 1-2 folds with MIC 25 µg/mL and 50 µg/mL respectively. Introduction of six member heterocyclic rings such as nicotinoyl (**6l**), picolinoyl (**6k**), 6-formicacid picolinoyl (**6n**) and isonicotinoyl groups (**6m**) at 4th position of **5** greatly enhanced the anti-TB activity by 4 – 16 folds with MIC 6.25 – 1.56 µg/mL. While, 2-(1H-indol-3-yl)acetyl (**6q**), 3-(1H-indol-3-yl)propanoyl (**6r**) and 4-(1H-indol-3-yl)butanoyl groups (**6s**) at 4th position of **5** witnessed either retention (**6q**) or greatly enhanced (**6r** and **6s**) the anti-TB activity by 1 – 16 folds. In conclusion, **6a-s** presence of EDGs on phenyl ring and five membered heterocyclic rings decreased anti-TB activity while EWGs, six membered and benzannulated heterocyclic rings increased the activity (exception **6d**).

SAR profile of the fourteen phenanthridine sulphonamide **(7a-n)** analogues is as follows. In the presence of simple methanesulfonyl group (**7a**) at the 4th position of compound **5** the anti-TB activity is retained with MIC 25 µg/mL. Benzenesulfonyl group (**7b**) at the 4th position of compound **5** increased the anti-TB activity by 4 fold with MIC 6.25 µg/mL. Presence of EDGs in the phenyl ring increased the activity in general exception being (**7c**). 2,4,6-triethyl groups (**7e**) on phenyl ring improved anti-TB activity by 2 fold with MIC 12.5 µg/mL. *Tert*-butyl group (**7d**) at para position on phenyl ring remarkably enriched the anti-TB activity by 16 folds with MIC 1.56 µg/mL. Methoxy group at para (**7k**) position on phenyl ring increased the anti-TB activity by 4 folds with MIC 6.25 µg/mL. Presence of electron withdrawing halogens (F (**7g**), Cl (**7h**) and Br (**7i**)) at para position on phenyl ring impressively enhanced the anti-TB activity by 4–8 folds with MIC 6.25 – 3.13 µg/mL, including compound **7f.** Electron withdrawing nitro (**7l**) and acetyl (**7m**) groups at para positions on phenyl ring either retained or decreased activity by 1–2 folds. 5-bromothiophene-2-sulfonyl group at 4th

position of 6-(piperazin-1-yl)phenanthridine (**5**) prominently augmented the anti-TB activity by 8 folds with MIC 3.13 µg/mL. In general, EWGs on phenyl ring enhanced or retained the anti-TB activity exception being **7l**. Wrapping up the results, we observe that in the series synthesized, sulphonamide analogues were more active than the amides.

3.2. Molecular modelling studies

To scrutinize the interaction profile, the compounds (**6b** and **7d)** were docked to the ATPase domain of MTB GyrB protein found from protein data bank (PDB ID–3ZKB) [23] with additional precision mode (XP) of Glide module [24]. The interaction patterns of the analogues were studied by starting with analysis of co-crystallized ligand docking pattern. The crystal ligand phosphoaminophosphonic acid-adenylate ester (ANP) was involved in prominent H-bonding connections, one of the interactions between the amino group of the ANP moiety and the oxygen atom of Asp79 at bond length was 1.78Å as shown in **Figure 2**. The direction of this ligand in the protein active site disclosed the presence of a hydrophobic pocket where the ANP moiety was stabilized by the interactions with val 99, Ile 84, lys 108 and Tyr 114. The docking pose of compounds **6b** and **7d** were portrayed in **figure 3** and **figure 4** respectively**.** Compound **6b** showed strong hydrogen bond interaction with Lys 108 by1.97Å distance. Both the compounds displayed common potent hydrophobic interactions with val 98, val 99, Ile 84, Pro 85, ala 113 and Tyr 114, whereas compound **7d** showed extra hydrophobic interaction with Ala 87 and strong π-π stacking interaction (CPK model of protein in **Figure 4**) with Arg 141. These hydrophobic interactions lead towards the specificity of compounds with this protein, assigning to its activity.

3.3. Cytotoxicity assay

Among the series, most active compounds (MIC ≤12.5 µg/mL) were subjected to Promega Cell Titer 96 non-radioactive cell proliferation assay to evaluate the *in vitro* cytotoxicity against mouse macrophage (RAW264.7) cell lines. The approximate IC_{50} values and selectivity index (SI) values [25] are tabulated in **Table 3.** In these all active compounds (MIC ≤12.5 µg/mL) displayed SI profile >7. while good anti-TB active compounds **6b**, **6e, 6k, 6n, 7h, 7i** and **7n** (MIC 3.13 µg/mL) exhibited SI profile >19. The most active anti-TB compounds **6m**, **6s**, and **7d** exhibited excellent SI profile >46. This outcome indicates that novel chemophores **6m**, **6s** and **7d** are not toxic and might be considered for further structural modification of phenanthridine piperazine amide/sulphonamide analogues as leads to accomplish the treatment of this deadly disease.

3.4. X-ray crystallographic study

The X-ray crystallographic analysis of the compounds **6b** and **7d** was carried out: Crystals were grown from the slow evaporation of a 1:3:6 ratio of methanol/dichloromethane/ethyl acetate solvent mixture at rt, to get white flake crystals. A desirable crystal under triclinic system with space groups $P\bar{1}$ of **6b,** crystal size/mm^3 0.6 × 0.5 × 0.4 and crystal under monoclinic system with space groups $P2_1/n$ of **7d,** crystal size/mm^3 0.6 × 0.5 × 0.4 respectively. These crystals were kept at 293 K during data collection. Using Computer programs SHELXL97 (Sheldrick, 2008) the structure was solved with the unknown structure solution program using unknown and refined with the SHELXS-97 (Sheldrick, 2008) [26]. The crystal data, data collection and structure refinement details are summarized in **Table 4** and molecular structure is given as an ORTEP diagram pictured in **Figure 5**. Crystallographic data of the compounds **6b** and **7d** were deposited with the Cambridge Crystallographic Data Centre (CCDC). These compounds have been assigned the following deposition numbers CCDC 1012376 and CCDC 1012377 respectively. The X-ray structure parameters and complete details of compound **6b** and **7d** are provided in supplementary material.

4. Conclusion:

In this communication, phenanthridine derivatives were synthesized with moderate to excellent yields. The preliminary *in vitro* anti-TB screening results, toxicity studies and SI profile results of compounds **6b**, **6e, 6k, 6n, 7h, 7i** and **7n** (MIC 3.13 µg/mL) displayed good anti-TB activity and SI profile >19. Compounds **6m**, **6s**, and **7d** (MIC 1.56 µg/mL) exhibited excellent anti-TB activity and SI profile >46. Detailed *in vivo* studies and the exact mechanistic studies of **6m**, **6s**, and **7d** analogues are scope of future study in our lab. The 6-(4-substitutedpiperazin-1-yl)phenanthridine skeleton is established to be an important motif for further development of anti-tubercular agents.

5. Experimental Section:

5.1. Materials and methods:

Chemicals and solvents were procured from commercial sources and are analytically pure. Thin-layer chromatography (TLC) was carried out on aluminium-supported silica gel plates (Merck 60 F254) with visualization of components by UV light (254 nm). Column chromatography was carried out on silica gel (Merck 230-400 mesh). ^{1}H NMR spectra and ^{13}C NMR spectra were recorded at 300 MHz using a Bruker AV 300 spectrometer or 400 MHz using a Bruker AV 400 spectrometer (Bruker CO., Switzerland) in $CDCl_3$ or DMSO-D_6 solution with tetramethylsilane as the internal standard, and chemical shift values (δ) were given in ppm. Microwave reactions were performed in closed vessel using Biotage Initiator

microwave synthesizer (Uppsala, Sweden). IR spectra were recorded on a FT-IR spectrometer (Schimadzu) and peaks are reported in cm^{-1}. Melting points were determined on an electro thermal melting point apparatus (Stuart-SMP30) in open capillary tubes and are uncorrected. Elemental analyses were analysed by Elementar Analysensysteme GmbH vario MICRO cube CHNS/O Analyzer. Mass spectra (ESI-MS) were recorded on Schimadzu MS/ESI mass spectrometer.

*5.2 Synthesis of title compounds (**6a-s** and **7a-n**)*

For **6a-s**: 6-(piperazin-1-yl)phenanthridine (1.14 mmol) was dissolved in DCM (4 mL) in an oven dry 25mL two necked RBF. TEA (3.41 mmol) and amide coupling reagent T_3P (1.36 mmol) followed by anhydrous substituted alkyl / aryl acids (1.14 mmol) were added at 0 ^oC and stirred at rt for 6h.

For **7a-n**: 6-(piperazin-1-yl)phenanthridine (1.14 mmol) was dissolved in DCM (4 mL) in an oven dry 25mL two necked RBF. TEA (3.41 mmol) followed by anhydrous substituted aryl sulfonyl chloride (1.36 mmol) were added at 0 ^oC and stirred for 2h at rt.

Completion of the reaction was monitored by TLC using 0 - 6% MeOH in DCM as mobile phase. After the reaction was complete, reaction mixture was quenched in ice cold water and extracted with DCM (3 x 10 mL), combined organic layers were washed with saturated brine solution and dried on anhydrous Na_2SO_4 then evaporated *in vacuo*. Obtained residue was purified by column chromatography using gradient 0 - 6% MeOH in DCM, to give the title compounds **(6a-s** and **7a-n)**.

5.2.1. 3-oxo-3-(4-(phenanthridin-6-yl)piperazin-1-yl)propanenitrile **(6a)**

Appearance: off white solid; yield = 78%; mp = 139-140 ^oC; ^1H NMR (400 MHz, $CDCl_3$) δ 8.56 (d, J = 8.4 Hz, 1H), 8.42 (d, J = 7.2 Hz, 1H), 8.02 (d, J = 8.4 Hz, 1H), 7.90 (d, J = 8.0 Hz, 1H), 7.82-7.48 (m, 4H), 3.82 – 3.54 (t, 8H), 3.46 (s, 2H). ^{13}C NMR (100.61 MHz, $CDCl_3$) δ 170.14, 161.68, 142.40, 136.22, 134.45, 131.41, 130.37, 128.83, 127.19, 125.14, 124.17, 122.13, 121.58, 120.26, 119.85, 51.60, 47.12, 31.28. FT-IR: ν 2248 (CN); ESI-MS: (m/z) calcd. for $C_{20}H_{18}N_4O$, 330.14, found: 331.22 $(M + H)^+$. Anal. Calcd for $C_{20}H_{18}N_4O$; (%) C 72.71, H 5.49, N 16.96; found: C 72.82, H 5.54, N 17.04.

5.2.2. (4-(phenanthridin-6-yl)piperazin-1-yl)(phenyl)methanone **(6b)**

Appearance: white solid; yield = 85%; mp = 108-109 ^oC; ^1H NMR (400 MHz, $CDCl_3$) δ 8.59 (d, J = 8.4 Hz, 1H), 8.46 (d, J = 7.2 Hz, 1H), 8.22 (d, J = 7.6 Hz, 1H), 7.91 (d, J = 8.0 Hz, 1H), 7.82 (t, J = 7.6 Hz, 1H), 7.78 (m, 2H), 7.66-7.45 (m, 6H), 4.12 – 3.51 (t, 8H). ^{13}C NMR (100.61 MHz, $CDCl_3$) δ 170.74, 159.62, 143.50, 135.74, 135.02, 133.41, 130.37, 130.12,

129.83, 128.83, 128.59, 127.15, 126.95, 126.14, 125.17, 122.83, 121.91, 121.26, 51.63, 47.82. ESI-MS: (m/z) calcd. for $C_{24}H_{21}N_3O$, 367.16, found: 368.23 $(M + H)^+$. Anal. Calcd for $C_{24}H_{21}N_3O$; (%) C 78.45, H 5.76, N 11.44; found: C 78.61, H 5.81, N 11.53.

5.2.3. (4-chlorophenyl)(4-(phenanthridin-6-yl)piperazin-1-yl)methanone **(6c)**

Appearance: off white solid; yield = 81%; mp = 132-133 ^oC; ^1H NMR (400 MHz, $CDCl_3$) δ 8.59 (d, J = 8.4 Hz, 1H), 8.46 (d, J = 8.8 Hz, 2H), 8.25 (d, J = 8.2 Hz, 1H), 7.96 (d, J = 10.8 Hz, 1H), 7.91 (d, J = 8.0 Hz, 1H), 7.84 (d, J = 8.8 Hz, 2H), 7.81 – 7.48 (m, 4H), 3.67 – 3.44 (t, 8H). ^{13}C NMR (100.61 MHz, $CDCl_3$) δ 170.52, 160.14, 144.22, 136.18, 135.81, 132.87, 131.08, 130.64, 129.54, 128.63, 128.32, 127.11, 126.84, 126.33, 125.46, 122.57, 121.87, 121.18, 52.28, 47.54. ESI-MS: (m/z) calcd. for $C_{24}H_{20}ClN_3O$, 401.12, found: 402.25 $(M + H)^+$. Anal. Calcd for $C_{24}H_{20}ClN_3O$; (%) C 71.73, H 5.02, N 10.46; found: C 71.81, H 5.09, N 10.53.

5.2.4. (4-nitrophenyl)(4-(phenanthridin-6-yl)piperazin-1-yl)methanone **(6d)**

Appearance: yellow solid; yield = 68%; mp = 148-149 ^oC; ^1H NMR (400 MHz, DMSO-d_6) δ 8.62 (d, J = 8.4 Hz, 1H), 8.48 (d, J = 8.0, 1H), 8.25 (d, J = 8.4 Hz, 1H), 8.20 (d, J = 9.6 Hz, 2H), 7.97 (d, J = 7.6 Hz, 1H), 7.92 (d, J = 8.0 Hz, 2H), 7.82 – 7.54 (m, 4H), 3.72 – 3.68 (t, 8H). ^{13}C NMR (100.61 MHz, DMSO-d_6) δ 172.12, 164.51, 146.86, 142.02, 139.53, 137.84, 132.07, 130.84, 129.74, 128.44, 128.01, 127.69, 126.80, 126.11, 125.47, 123.78, 122.35, 120.88, 52.23, 48.59. ESI-MS: (m/z) calcd. for $C_{24}H_{20}N_4O_3$, 412.15, found: 413.22 $(M + H)^+$. Anal. Calcd for $C_{24}H_{20}N_4O_3$; (%) C 69.89, H 4.89, N 13.58; found: C 69.98, H 4.95, N 13.70.

5.2.5. (3-nitrophenyl)(4-(phenanthridin-6-yl)piperazin-1-yl)methanone **(6e)**

Appearance: pale yellow solid; yield = 63%; mp = 230-231 ^oC; ^1H NMR (400 MHz, DMSO-d_6) δ 8.69 (s, 1H), 8.63 (d, J = 8.4 Hz, 1H), 8.42 (d, J = 8.0, 1H), 8.26 (d, J = 8.4 Hz, 1H), 8.21 (d, J = 9.2 Hz, 1H), 7.97 (d, J = 7.6 Hz, 1H), 7.93 (m, 1H), 7.92 (d, J = 8.0 Hz, 1H), 7.82 – 7.54 (m, 4H), 3.69 – 3.57 (t, 8H). ^{13}C NMR (100.61 MHz, DMSO-d_6) δ 171.08, 162.31, 147.36, 143.47, 141.11, 139.62, 135.24, 132.04, 131.84, 130.02, 129.21, 128.68, 128.32, 127.34, 126.01, 125.82, 125.21, 123.52, 121.76, 120.88, 53.62, 47.84. ESI-MS: (m/z) calcd. for $C_{24}H_{20}N_4O_3$, 412.15, found: 413.20 $(M + H)^+$. Anal. Calcd for $C_{24}H_{20}N_4O_3$; (%) C 69.89, H 4.89, N 13.58; found: C 69.96, H 4.96, N 13.66.

5.2.6. (3,5-dinitrophenyl)(4-(phenanthridin-6-yl)piperazin-1-yl)methanone **(6f)**

Appearance: yellow solid; yield = 64%; mp = 196-197 ^oC; ^1H NMR (400 MHz, DMSO-d_6) δ 9.08 – 8.83 (s, 3H), 8.46 (d, J = 8.0, 1H), 8.22 (d, J = 8.4 Hz, 1H), 8.18 (d, J = 7.6 Hz, 1H),

7.93 (d, *J* = 8.0 Hz, 1H), 7.85 – 7.48 (m, 4H), 3.71 – 3.62 (t, 8H). ^{13}C NMR (100.61 MHz, DMSO-d_6) δ 172.32, 159.22, 154.08, 144.75, 142.47, 139.81, 138.02, 133.83, 132.38, 130.39, 129.21, 128.52, 127.01, 125.44, 124.23, 122.89, 121.22, 119.65, 52.63, 47.82. ESI-MS: (m/z) calcd. for $C_{24}H_{19}N_5O_5$, 457.13, found: 458.21 $(M + H)^+$. Anal. Calcd for $C_{24}H_{19}N_5O_5$; (%) C 63.02, H 4.19, N 15.31; found: C 63.11, H 4.24, N 15.39.

5.2.7. (2-aminophenyl)(4-(phenanthridin-6-yl)piperazin-1-yl)methanone **(6g)**

Appearance: white solid; yield = 60%; mp = 164-165 ^{o}C; ^{1}H NMR (400 MHz, DMSO-d_6) δ 8.38 (d, *J* = 8.0 Hz, 1H), 8.22 (d, *J* = 7.6 Hz, 1H), 8.07 (d, *J* = 8.0 Hz, 1H), 7.91 (d, *J* = 8.4 Hz, 1H), 7.80 – 7.18 (m, 6H), 7.12 (d, *J* = 8.4 Hz, 1H), 7.09 (d, *J* = 8.4 Hz, 1H), 6.02 (br, 2H), 3.68 – 3.52 (t, 8H). ^{13}C NMR (100.61 MHz, DMSO-d_6) δ 169.78, 158.13, 146.87, 142.42, 141.44, 138.23, 137.54, 131.12, 130.66, 130.08, 129.23, 128.84, 126.45, 124.87, 124.12, 123.88, 121.86, 120.22, 119.82, 118.52, 52.42, 46.57. ESI-MS: (m/z) calcd. for $C_{24}H_{22}N_4O$, 382.17, found: 383.26 $(M + H)^+$. Anal. Calcd for $C_{24}H_{22}N_4O$; (%) C 75.37, H 5.80, N 14.65; found: C 75.51, H 5.85, N 14.54.

5.2.8. (4-aminophenyl)(4-(phenanthridin-6-yl)piperazin-1-yl)methanone **(6h)**

Appearance: off white semi solid; yield = 62%; mp = Not determined (ND); ^{1}H NMR (400 MHz, DMSO-d_6) δ 8.57 (d, *J* = 8.4 Hz, 1H), 8.43 (d, *J* = 8.0, 1H), 8.22 (d, *J* = 7.8 Hz, 1H), 7.98 (d, *J* = 8.4 Hz, 1H), 7.84 (m, 1H), 7.74 (d, *J* = 8.4 Hz, 2H), 7.71 – 7.52 (m, 3H), 7.18 (d, *J* = 8.2 Hz, 2H), 5.84 (br, 2H), 3.78 – 3.54 (t, 8H). ^{13}C NMR (100.61 MHz, DMSO-d_6) δ 170.84, 163.58, 147.18, 146.09, 140.25, 134.28, 131.12, 130.82, 129.98, 128.22, 127.84, 127.02, 126.45, 125.34, 124.72, 123.21, 122.87, 119.24, 52.64, 47.82. ESI-MS: (m/z) calcd. for $C_{24}H_{22}N_4O$, 382.17, found: 383.22 $(M + H)^+$. Anal. Calcd for $C_{24}H_{22}N_4O$; (%) C 75.37, H 5.80, N 14.65; found: C 75.54, H 5.86, N 14.52.

5.2.9. 2-(naphthalen-1-yl)-1-(4-(phenanthridin-6-yl)piperazin-1-yl)ethanone **(6i)**

Appearance: pale yellow solid; yield = 75%; mp = 181-182 ^{o}C; ^{1}H NMR (400 MHz, DMSO-d_6) δ 8.80 (d, *J* = 8.4 Hz, 1H), 8.65 (d, *J* = 8.0 Hz, 1H), 8.28 (d, *J* = 8.8 Hz, 1H), 8.14 (d, *J* = 8.0 Hz, 1H), 7.96 (d, *J* = 7.8 Hz, 1H), 7.91 (d, *J* = 8.0 Hz, 1H), 7.82 (d, *J* = 7.6 Hz, 1H), 7.78 – 7.42 (m, 7H), 7.31 (d, *J* = 8.0 Hz, 1H), 4.28 (s, 2H), 3.93 – 3.40 (t, 8H). ^{13}C NMR (100.61 MHz, DMSO-d_6) δ 172.09, 163.24, 150.86, 148.13, 141.18, 140.45, 138.16, 134.22, 133.72, 132.07, 131.28, 130.88, 129.12, 128.33, 126.57, 125.78, 124.02, 123.31, 123.04, 122.89, 122.23, 121.64, 121.02, 120.58, 50.82, 48.54. ESI-MS: (m/z) calcd. for $C_{29}H_{25}N_3O$, 431.19, found: 432.33 $(M + H)^+$. Anal. Calcd for $C_{29}H_{25}N_3O$; (%) C 80.72, H 5.84, N 9.74; found: C 80.79, H 5.87, N 9.81.

5.2.10. (E)-1-(4-(phenanthridin-6-yl)piperazin-1-yl)-3-phenylprop-2-en-1-one **(6j)**

Appearance: off white greenish solid; yield = 72%; mp = 154-156 ^{o}C; ^{1}H NMR (400 MHz, DMSO-d_6) δ 8.58 (d, J = 8.4 Hz, 1H), 8.24 (d, J = 8.0 Hz, 1H), 8.08 (d, J = 7.8 Hz, 1H), 7.88 (d, J = 8.0 Hz, 1H), 7.79 (d, J = 8.0 Hz, 2H), 7.75 – 7.48 (m, 7H), 7.38 (d, J = 15.2 Hz, 1H), 7.29 (d, J = 15.8 Hz, 1H), 3.68 – 3.54 (t, 8H). ^{13}C NMR (100.61 MHz, DMSO-d_6) δ 172.08, 161.22, 154.16, 148.12, 140.82, 138.45, 133.16, 132.84, 131.90, 128.37, 127.78, 125.23, 124.88, 123.65, 122.44, 122.21, 121.84, 121.22, 120.36, 118.41, 51.59, 46.38. ESI-MS: (m/z) calcd. for $C_{26}H_{23}N_3O$, 393.18, found: 394.27 $(M + H)^+$. Anal. Calcd for $C_{26}H_{23}N_3O$; (%) C 79.36, H 5.89, N 10.68; found: C 79.48, H 5.93, N 10.75.

5.2.11. (4-(phenanthridin-6-yl)piperazin-1-yl)(pyridin-2-yl)methanone **(6k)**

Appearance: off white semi solid; yield = 78%; mp = ND; ^{1}H NMR (400 MHz, $CDCl_3$) δ 8.59 (d, J = 8.8 Hz, 1H), 8.46 (d, J = 8.4 Hz, 1H), 8.25 (d, J = 8.8 Hz, 1H), 8.14 (m, 1H), 7.96 (d, J = 7.8 Hz, 1H), 7.91 (d, J = 8.0 Hz, 1H), 7.82 (d, J = 7.6 Hz, 1H), 7.78 – 7.48 (m, 5H), 3.92 – 3.52 (t, 8H). ^{13}C NMR (100.61 MHz, $CDCl_3$) δ 171.23, 160.89, 154.04, 151.12, 149.34, 142.81, 140.86, 133.17, 132.34, 130.14, 129.13, 128.47, 126.05, 124.60, 123.37, 122.88, 122.14, 121.22, 120.80, 51.74, 46.58. ESI-MS: (m/z) calcd. for $C_{23}H_{20}N_4O$, 368.16, found: 369.24 $(M + H)^+$. Anal. Calcd for $C_{23}H_{20}N_4O$; (%) C 74.98, H 5.47, N 15.21; found: C 75.07, H 5.41, N 15.14.

5.2.12. (4-(phenanthridin-6-yl)piperazin-1-yl)(pyridin-3-yl)methanone **(6l)**

Appearance: off white solid; yield = 74%; mp = 153-154 ^{o}C; ^{1}H NMR (400 MHz, DMSO-d_6) δ 8.81 (s, 1H), 8.72 (d, J = 8.4 Hz, 2H), 8.64 (d, J = 8.0 Hz, 1H), 8.28 (d, J = 8.8 Hz, 1H), 7.94 (m, 2H), 7.83 (d, J = 8.0 Hz, 1H), 7.78 – 7.51 (m, 4H), 3.98 – 3.44 (t, 8H). ^{13}C NMR (100.61 MHz, DMSO-d_6) δ 170.84, 162.45, 153.76, 153.23, 151.88, 141.54, 139.72, 132.65, 132.11, 130.81, 129.33, 128.28, 126.32, 124.86, 123.42, 122.46, 122.02, 121.85, 120.43, 52.68, 47.54. ESI-MS: (m/z) calcd. for $C_{23}H_{20}N_4O$, 368.16, found: 369.28 $(M + H)^+$. Anal. Calcd for $C_{23}H_{20}N_4O$; (%) C 74.98, H 5.47, N 15.21; found: C 75.05, H 5.45, N 15.12.

5.2.13. (4-(phenanthridin-6-yl)piperazin-1-yl)(pyridin-4-yl)methanone **(6m)**

Appearance: off white semi solid; yield = 81%; mp = ND; ^{1}H NMR (400 MHz, $CDCl_3$) δ 8.74 (d, J = 8.8 Hz, 2H), 8.45 (d, J = 8.0 Hz, 1H), 8.18 (d, J = 8.4 Hz, 1H), 7.96 (d, J = 7.8 Hz, 1H), 7.92 (d, J = 8.4 Hz, 2H), 7.82 (d, J = 7.6 Hz, 1H), 7.75 – 7.44 (m, 4H), 3.88 – 3.54 (t, 8H). ^{13}C NMR (100.61 MHz, $CDCl_3$) δ 172.06, 159.15, 152.74, 150.89, 147.21, 144.39, 139.82, 133.45, 130.23, 128.06, 127.14, 126.23, 124.18, 123.42, 122.01, 121.79, 120.12,

52.36, 47.52. ESI-MS: (m/z) calcd. for $C_{23}H_{20}N_4O$, 368.16, found: 369.23 $(M + H)^+$. Anal. Calcd for $C_{23}H_{20}N_4O$; (%) C 74.98, H 5.47, N 15.21; found: C 75.12, H 5.40, N 15.16.

5.2.14. 6-(4-(phenanthridin-6-yl)piperazine-1-carbonyl)picolinic acid **(6n)**

Appearance: off white semi solid; yield = 65%; mp = ND; ^{1}H NMR (400 MHz, DMSO-d_6) δ 11.58 (s, 1H), 8.88 (d, *J* = 8.4 Hz, 1H), 8.82 (d, *J* = 9.2 Hz, 1H), 8.61 (m, 1H), 8.57 (d, *J* = 8.4 Hz, 1H), 8.26 (d, *J* = 8.0 Hz, 1H), 8.04 (d, *J* = 8.4 Hz, 1H), 7.87 (d, *J* = 7.8 Hz, 1H), 7.79 – 7.46 (m, 4H), 3.82 – 3.52 (t, 8H). ^{13}C NMR (100.61 MHz, DMSO-d_6) δ 172.36, 171.81, 160.12, 152.45, 150.86, 148.32, 143.75, 140.48, 135.08, 134.53, 131.24, 129.04, 128.14, 126.87, 124.12, 123.44, 122.81, 122.63, 121.07, 120.24, 52.72, 47.50. ESI-MS: (m/z) calcd. for $C_{24}H_{20}N_4O_3$, 412.15, found: 413.28 $(M + H)^+$. Anal. Calcd for $C_{24}H_{20}N_4O_3$; (%) C 69.89, H 4.89, N 13.58; found: C 69.98, H 4.95, N 13.64.

5.2.15. furan-2-yl(4-(phenanthridin-6-yl)piperazin-1-yl)methanone **(6o)**

Appearance: off white solid; yield = 76%; mp = 118-119 ^{o}C; ^{1}H NMR (400 MHz, $CDCl_3$) δ 8.59 (d, *J* = 8.8 Hz, 1H), 8.44 (d, *J* = 8.0 Hz, 1H), 8.18 (d, *J* = 8.4 Hz, 1H), 8.02 (d, *J* = 8.8 Hz, 1H), 7.92 (d, *J* = 8.0 Hz, 1H), 7.86 – 7.54 (m, 4H), 7.43 (d, *J* = 7.8 Hz, 1H), 7.22 (m, 1H), 4.94 – 3.68 (t, 8H). ^{13}C NMR (100.61 MHz, $CDCl_3$) δ 169.74, 157.68, 148.15, 142.44, 135.22, 133.45, 130.87, 130.12, 129.18, 128.84, 128.04, 127.21, 126.90, 126.12, 125.18, 122.18, 121.98, 118.24, 51.68, 48.84. ESI-MS: (m/z) calcd. for $C_{22}H_{19}N_3O_2$, 357.14, found: 358.25 $(M + H)^+$. Anal. Calcd for $C_{22}H_{19}N_3O_2$; (%) C 73.93, H 5.36, N 11.76; found: C 73.99, H 5.41, N 11.83.

5.2.16. (4-(phenanthridin-6-yl)piperazin-1-yl)(thiophen-2-yl)methanone **(6p)**

Appearance: white solid; yield = 81%; mp = 143-145 ^{o}C; ^{1}H NMR (400 MHz, DMSO-d_6) δ 8.72 (d, *J* = 8.8 Hz, 1H), 8.58 (d, *J* = 8.0 Hz, 1H), 8.42 (d, *J* = 8.0 Hz, 1H), 8.23 (d, *J* = 8.0 Hz, 1H), 8.08 (d, *J* = 8.4 Hz, 1H), 7.90 (d, *J* = 8.0 Hz, 1H), 7.88 – 7.37 (m, 5H), 4.89 – 3.53 (t, 8H). ^{13}C NMR (100.61 MHz, DMSO-d_6) δ 170.02, 158.88, 149.22, 141.89, 136.72, 131.93, 130.12, 129.94, 129.34, 128.84, 128.11, 127.26, 126.95, 125.87, 125.03, 122.48, 121.68, 120.87, 52.46, 47.52. ESI-MS: (m/z) calcd. for $C_{22}H_{19}N_3OS$, 373.12, found: 374.27 $(M + H)^+$. Anal. Calcd for $C_{22}H_{19}N_3OS$; (%) C 70.75, H 5.13, N 11.25; found: C 70.83, H 5.19, N 11.15.

5.2.17. 2-(1H-indol-3-yl)-1-(4-(phenanthridin-6-yl)piperazin-1-yl)ethanone **(6q)**

Appearance: off white solid; yield = 80%; mp = 162-163 ^{o}C; ^{1}H NMR (400 MHz, DMSO-d_6) δ 8.24 (d, *J* = 8.0 Hz, 1H), 8.08 (d, *J* = 7.6 Hz, 1H), 7.91 (d, *J* = 8.0 Hz, 1H), 7.88 (d, *J* = 8.0 Hz, 1H), 7.84 (m, 1H), 7.79 (d, *J* = 7.2 Hz, 1H), 7.58 – 7.48 (m, 3H), 7.42 (d, *J* = 8.0 Hz,

1H), 7.34 (s, 1H), 7.20 (m, 2H), 6.08 (br, 1H), 3.88 (t, 4H), 3.80 (s, 2H), 3.52 (t, 4H). ^{13}C NMR (100.61 MHz, DMSO-d_6) δ 168.54, 159.62, 144.83, 143.23, 140.23, 138.64, 135.49, 135.05, 133.63, 132.84, 129.47, 128.43, 127.19, 126.82, 126.11, 124.46, 123.23, 121.52, 119.88, 119.04, 117.74, 108.04, 52.64, 48.48, 40.68. ESI-MS: (m/z) calcd. for $C_{27}H_{24}N_4O$ 420.19, found: 421.15 $(M + H)^+$. Anal. Calcd for $C_{27}H_{24}N_4O$: (%) C 77.12, H 5.75, N 13.32; Found: C 77.24, H 5.88, N 13.41.

5.2.18. 3-(1H-indol-3-yl)-1-(4-(phenanthridin-6-yl)piperazin-1-yl)propan-1-one **(6r)**

Appearance: off white solid; yield = 83%; mp = 120-121 ^{o}C; ^{1}H NMR (400 MHz, DMSO-d_6) δ 8.19 (d, J = 8.0 Hz, 1H), 8.02 (d, J = 7.8 Hz, 1H), 7.94 (d, J = 7.6 Hz, 1H), 7.86 (d, J = 7.2 Hz, 1H), 7.80 (m, 1H), 7.76 (d, J = 7.8 Hz, 1H), 7.61 – 7.44 (m, 3H), 7.41 (d, J = 8.0 Hz, 1H), 7.38 (s, 1H), 7.22 (m, 2H), 6.84 (br, 1H), 3.92 – 2.70 (t, 12H). ^{13}C NMR (100.61 MHz, DMSO-d_6) δ 170.22, 162.48, 145.16, 144.06, 141.18, 139.21, 136.42, 135.84, 133.82, 133.08, 128.92, 128.11, 127.64, 126.74, 126.32, 124.22, 123.68, 120.94, 119.24, 118.48, 117.38, 110.28 52.12, 47.39, 39.94, 32.98. ESI-MS: (m/z) calcd. for $C_{28}H_{26}N_4O$ 434.21, found: 435.28 $(M + H)^+$. Anal. Calcd for $C_{28}H_{26}N_4O$: (%) C 77.39, H 6.03, N 12.89; Found: C 77.46, H 6.12, N 12.94.

5.2.19. 4-(1H-indol-3-yl)-1-(4-(phenanthridin-6-yl)piperazin-1-yl)butan-1-one **(6s)**

Appearance: off white solid; yield = 75%; mp = 148-149 ^{o}C; ^{1}H NMR (400 MHz, DMSO-d_6) δ 8.22 (d, J = 8.0 Hz, 1H), 8.07 (d, J = 7.6 Hz, 1H), 7.98 (d, J = 7.8 Hz, 1H), 7.89 (d, J = 7.4 Hz, 1H), 7.84 (m, 1H), 7.72 (d, J = 7.4 Hz, 1H), 7.62 – 7.39 (m, 3H), 7.35 (d, J = 8.0 Hz, 1H), 7.30 (s, 1H), 7.18 (m, 2H), 6.42 (br, 1H), 3.89 – 2.60 (t, 12H), 1.68 (m, 2H). ^{13}C NMR (100.61 MHz, DMSO-d_6) δ 170.84, 163.04, 144.87, 143.21, 141.85, 139.42, 135.08, 134.91, 133.09, 132.44, 129.48, 128.74, 127.04, 126.23, 123.11, 122.41, 122.26, 121.39, 120.12, 119.94, 118.87, 111.46, 52.88, 46.24, 40.37, 30.42, 39.87. ESI-MS: (m/z) calcd. for $C_{29}H_{28}N_4O$ 448.22, found: 449.24 $(M + H)^+$. Anal. Calcd for $C_{29}H_{28}N_4O$: (%) C 77.65, H 6.29, N 12.49; Found: C 77.72, H 6.38, N 12.38.

5.2.20. 6-(4-(methylsulfonyl)piperazin-1-yl)Phenanthridine **(7a)**:

Appearance: off white semi solid; yield = 78%; mp = ND; ^{1}H NMR (400 MHz, $CDCl_3$) δ 8.26 (d, J = 8.0 Hz, 1H), 8.13 (d, J = 7.8 Hz, 1H), 7.97 (d, J = 8.0 Hz, 1H), 7.81 (d, J = 7.4 Hz, 1H), 7.74 – 7.41 (m, 4H), 3.87 – 3.53 (t, 8H), 3.09 (s, 3H). ^{13}C NMR (100.61 MHz, $CDCl_3$) δ 164.24, 148.76, 140.08, 133.13, 131.67, 130.43, 129.88, 123.24, 122.41, 121.82, 120.34, 119.92, 114.34, 53.65, 48.21, 38.98. ESI-MS: (m/z) calcd. for $C_{18}H_{19}N_3O_2S$ 341.12,

found: 342.14 $(M + H)^+$. Anal. Calcd for $C_{18}H_{19}N_3O_2S$: (%) C 63.32, H 5.61, N 12.31; found: C 63.64, H 5.74, N 12.28.

5.2.21. 6-(4-(phenylsulfonyl)piperazin-1-yl)phenanthridine **(7b)**

Appearance: off white solid; yield = 88%; mp = 238-239 ^oC; ^1H NMR (400 MHz, $CDCl_3$) δ 8.57 (d, J = 8.0 Hz, 1H), 8.41 (d, J = 7.6 Hz, 1H), 8.02 (d, J = 7.8 Hz, 2H), 7.90 (dd, J = 9.0 Hz, J = 0.8 Hz, 1H), 7.82 (d, J = 7.4 Hz, 1H), 7.77 – 7.39 (m, 7H), 3.68 – 3.44 (t, 8H). ^{13}C NMR (100.61 MHz, $CDCl_3$) δ 162.86, 152.08, 141.12, 138.47, 132.24, 131.82, 130.12, 129.64, 124.28, 123.81, 122.89, 121.24, 121.08, 120.42, 119.92, 118.42, 112.47, 50.48, 48.07. ESI-MS: (m/z) calcd. for $C_{23}H_{21}N_3O_2S$ 403.13, found: 403.22 $(M + H)^+$. Anal. Calcd for $C_{23}H_{21}N_3O_2S$: (%) C 68.46, H 5.25, N 10.41; found: C 68.55, H 5.32, N 10.60.

5.2.22. 6-(4-tosylpiperazin-1-yl)phenanthridine **(7c)**

Appearance: pale yellow solid; yield = 93%; mp = 188-189 ^oC; ^1H NMR (400 MHz, $CDCl_3$) δ 8.48 (d, J = 8.2 Hz, 1H), 8.01 (d, J = 7.6 Hz, 1H), 7.91 (dd, J = 8.4 Hz, J = 0.8 Hz, 1H), 7.88 (d, J = 8.4 Hz, 1H), 7.80 (d, J = 7.8 Hz, 2H), 7.79 (d, J = 8.0 Hz, 2H), 7.74 – 7.46 (m, 4H), 3.64 – 3.38 (t, 8H), 2.94 (s, 3H). ^{13}C NMR (100.61 MHz, $CDCl_3$) δ 162.42, 153.14, 144.46, 139.08, 138.81, 132.11, 131.81, 129.64, 128.43, 124.82, 123.08, 122.28, 121.63, 120.42, 119.92, 118.42, 113.22, 52.18, 47.11, 24.08. ESI-MS: (m/z) calcd. for $C_{24}H_{23}N_3O_2S$ 417.15, found: 417.24 $(M + H)^+$. Anal. Calcd for $C_{24}H_{23}N_3O_2S$: (%) C 69.04, H 5.55, N 10.06; found: C 69.11, H 5.64, N 10.12.

5.2.23. 6-(4-(4-tert-butylphenylsulfonyl)piperazin-1-yl)phenanthridine **(7d)**

Appearance: white solid; yield = 88%; mp = 154-155 ^oC; ^1H NMR (400 MHz, $CDCl_3$) δ 8.58 (d, J = 8.0 Hz, 1H), 8.45 (d, J = 8.2 Hz, 1H), 8.04 (d, J = 8.0 Hz, 1H), 7.91 (dd, J = 8.4 Hz, J = 0.8 Hz, 1H), 7.78 (dd, J = 6.4 Hz, J = 1.6 Hz, 1H), 7.74 (dd, J = 8.8 Hz, J = 1.6 Hz, 1H), 7.76 (m, 1H), 7.74 (d, J = 7.2 Hz, 1H), 7.64 – 7.55 (m, 4H), 7.51 (d, J = 8.0 Hz, 1H), 3.60 – 3.35 (t, 8H), 1.37 (s, 9H). ^{13}C NMR (100.61 MHz, $CDCl_3$) δ 159.24, 156.71, 143.45, 134.98, 132.83, 130.30, 128.82, 128.62, 127.79, 126.81, 126.17, 125.95, 125.14, 122.85, 122.65, 121.86, 121.03, 50.48, 46.03, 35.23, 31.13. ESI-MS: (m/z) calcd. for $C_{27}H_{29}N_3O_2S$ 459.19, found: 460.25 $(M + H)^+$. Anal. Calcd for $C_{27}H_{29}N_3O_2S$: (%) C 70.56, H 6.36, N 9.14; found: C 70.64, H 6.28, N 9.24.

5.2.24. 6-(4-(mesitylsulfonyl)piperazin-1-yl)phenanthridine **(7e)**

Appearance: white solid; yield = 81%; mp = 118-119 ^oC; ^1H NMR (400 MHz, $CDCl_3$) δ 8.48 (d, J = 8.0 Hz, 1H), 8.24 (d, J = 8.0 Hz, 1H), 7.98 (dd, J = 8.8 Hz, J = 1.6 Hz, 1H), 7.82 (dd, J = 7.2 Hz, J = 1.2 Hz, 1H), 7.72 – 7.58 (m, 4H), 7.24 (s, 2H), 3.62 – 3.42 (t, 8H), 2.88 – 2.62

(s, 9H). ^{13}C NMR (100.61 MHz, $CDCl_3$) δ 162.38, 157.24, 148.12, 145.31, 139.45, 138.08, 131.78, 131.41, 130.21, 127.09, 125.22, 124.62, 123.26, 122.08, 121.96, 121.14, 120.42, 51.04, 47.21, 31.08, 30.88. ESI-MS: (m/z) calcd. for $C_{26}H_{27}N_3O_2S$, 445.18, found: 446.23 $(M + H)^+$. Anal. Calcd for $C_{26}H_{27}N_3O_2S$; (%) C 70.08, H 6.11, N 9.43; found: C 70.14, H 6.23, N 9.59.

5.2.25. 6-(4-(4-chloro-2,5-dimethylphenylsulfonyl)piperazin-1-yl)phenanthridine **(7f)**

Appearance: white solid; yield = 87%; mp = 163-164 ^{o}C; ^{1}H NMR (400 MHz, $CDCl_3$) δ 8.58 (d, J = 8.4 Hz, 1H), 8.46 (d, J = 8.0 Hz, 1H), 8.12 (d, J = 8.8 Hz, 1H), 7.91 (d, J = 7.8 Hz, 1H), 7.85 (s, 1H), 7.78 – 7.53 (m, 4H), 7.34 (s, 1H), 3.56 – 3.46 (t, 8H), 2.62 – 2.42 (s, 6H). ^{13}C NMR (100.61 MHz, $CDCl_3$) δ 164.21, 158.73, 149.08, 142.74, 141.03, 139.22, 137.63, 137.24, 134.09, 131.11, 130.87, 129.32, 128.08, 126.43, 123.28, 122.92, 121.03, 120.25, 119.46, 51.82, 47.04, 36.42, 30.12. ESI-MS: (m/z) calcd. for $C_{25}H_{24}ClN_3O_2S$, 465.12, found: 466.15 $(M + H)^+$. Anal. Calcd for $C_{25}H_{24}ClN_3O_2S$; (%) C 64.44, H 5.19, N 9.02; found: C 64.58, H 5.30, N 9.14.

5.2.26. 6-(4-(4-fluorophenylsulfonyl)piperazin-1-yl)phenanthridine **(7g)**

Appearance: pale yellow solid; yield = 74%; mp = 188-189 ^{o}C; ^{1}H NMR (400 MHz, $CDCl_3$) δ 8.57 (d, J = 8.2 Hz, 1H), 8.42 (d, J = 8.0 Hz, 1H), 8.03 (d, J = 8.2 Hz, 1H), 7.90 (d, J = 8.2 Hz, 1H), 7.48 – 7.29 (m, 8H), 3.64 – 3.32 (t, 8H). ^{13}C NMR (100.61 MHz, $CDCl_3$) δ 161.86, 160.08, 151.11, 149.23, 138.14, 137.67, 135.62, 132.16, 131.23, 128.32, 126.45, 124.82, 123.88, 122.44, 121.21, 120.08, 114.05, 52.24, 46.42. ESI-MS: (m/z) calcd. for $C_{23}H_{20}FN_3O_2S$, 421.12, found: 422.25 $(M + H)^+$. Anal. Calcd for $C_{23}H_{20}FN_3O_2S$; (%) C 65.54, H 4.78, N 9.97; found: C 65.62, H 4.88, N 10.08.

5.2.27. 6-(4-(4-chlorophenylsulfonyl)piperazin-1-yl)phenanthridine **(7h)**

Appearance: white solid; yield = 82%; mp = 196-197 ^{o}C; ^{1}H NMR (400 MHz, $CDCl_3$) δ 8.59 (d, J = 10.8 Hz, 1H), 8.46 (dd, J = 10.8 Hz, J = 1.6 Hz 1H), 8.25 (dd, J = 11.2 Hz, J = 1.2 Hz 1H), 7.96 (dd, J = 10.8 Hz, J = 1.2 Hz 1H), 7.82 – 7.48 (m, 4H), 7.28 (d, J = 6.8 Hz, 1H), 7.24 (d, J = 7.2 Hz, 1H), 3.67 – 3.44 (t, 8H). ^{13}C NMR (100.61 MHz, $CDCl_3$) δ 163.14, 159.28, 150.88, 142.23, 139.86, 134.07, 132.47, 131.52, 129.71, 128.91, 127.20, 124.88, 124.25, 123.62, 122.89, 121.03, 120.21, 51.72, 46.05. ESI-MS: (m/z) calcd. for $C_{23}H_{20}ClN_3O_2S$; 437.09, found: 438.15 $(M + H)^+$. Anal. Calcd for $C_{23}H_{20}ClN_3O_2S$; (%) C 63.08, H4.60, N 9.59; found: 63.19, H4.64, N 9.65.

5.2.28. 6-(4-(4-bromophenylsulfonyl)piperazin-1-yl)phenanthridine **(7i)**

Appearance: pale yellow solid; yield = 78%; mp = 224-225 ^{o}C; ^{1}H NMR (400 MHz, $CDCl_3$) δ 8.64 (d, J = 8.4 Hz, 1H), 8.61 (d, J = 7.6 Hz, 1H), 8.08 (d, J = 8.4 Hz, 1H), 7.88 (m, 1H), 7.84 (d, J = 7.2 Hz, 1H), 7.82 – 7.51 (m, 5H), 7.22 (d, J = 7.2 Hz, 2H), 3.51 – 3.20 (t, 8H). ^{13}C NMR (100.61 MHz, $CDCl_3$) δ 163.80, 159.12, 148.46, 144.02, 139.14, 138.07, 134.61, 133.72, 131.98, 131.34, 127.45, 126.82, 123.74, 122.46, 121.84, 121.03, 120.42, 51.68, 47.04. ESI-MS: (m/z) calcd. for $C_{23}H_{20}BrN_3O_2S$, 481.04, found: 482.13 $(M + H)^+$. Anal. Calcd for $C_{23}H_{20}BrN_3O_2S$; (%) C 57.27, H 4.18, N 8.71; found: C 57.34, H 4.23, N 8.85.

5.2.29. 6-(4-(4-(trifluoromethyl)phenylsulfonyl)piperazin-1-yl)phenanthridine **(7j)**

Appearance: pale yellow solid; yield = 74%; mp = 163-164 ^{o}C; ^{1}H NMR (400 MHz, $CDCl_3$) δ 8.57 (d, J = 8.2 Hz, 1H), 8.44 (d, J = 7.6 Hz, 1H), 8.02 (d, J = 8.4 Hz, 1H), 7.98 – 7.49 (m, 9H), 3.63 – 3.38 (t, 8H). ^{13}C NMR (100.61 MHz, $CDCl_3$) δ 161.24, 156.68, 149.12, 142.81, 138.37, 134.12, 131.28, 130.98, 130.12, 129.35, 128.84, 128.02, 126.87, 124.07, 123.89, 121.25, 120.81, 119.48, 52.38, 48.65. ESI-MS: (m/z) calcd. for $C_{24}H_{20}F_3N_3O_2S$; 471.12, found: 472.18 $(M + H)^+$. Anal. Calcd for $C_{24}H_{20}F_3N_3O_2S$; (%) C 61.14, H 4.28, N 8.91; found: C 61.18, H 4.31, N 8.86.

5.2.30. 6-(4-(4-methoxyphenylsulfonyl)piperazin-1-yl)phenanthridine **(7k)**

Appearance: pale yellow solid; yield = 78%; mp = 208-209 ^{o}C; ^{1}H NMR (400 MHz, $CDCl_3$) δ 8.76 (d, J = 8.4 Hz, 1H), 8.63 (d, J = 7.6 Hz, 1H), 8.09 (d, J = 8.4 Hz, 1H), 7.88 (m, 1H), 7.82 (dd, J = 8.4 Hz, J = 1.2 Hz, 1H), 7.78 – 7.74 (m, 2H), 7.69 (dd, J = 8.0 Hz, J = 0.8 Hz, 1H), 7.65 (dd, J = 8.0 Hz, J = 0.8 Hz, 1H), 7.55 (m, 1H), 7.22 (d, J = 7.2 Hz, 2H), 3.88 (s, 3H), 3.47 – 3.32 (t, 8H). ^{13}C NMR (100.61 MHz, $CDCl_3$) δ 164.08, 160.28, 151.42, 140.23, 133.86, 132.46, 131.27, 130.52, 128.74, 127.91, 126.24, 124.88, 124.21, 123.63, 122.87, 120.03, 118.77, 51.78, 46.53. ESI-MS: (m/z) calcd. for $C_{24}H_{23}N_3O_3S$; 433.14, found: 434.23 $(M + H)^+$. Anal. Calcd for $C_{24}H_{23}N_3O_3S$; (%) C 66.49, H 5.35, N 9.69; found: C 66.54, H 5.42, N 9.77.

5.2.31. 6-(4-(4-nitrophenylsulfonyl)piperazin-1-yl)phenanthridine **(7l)**

Appearance: pale yellow solid; yield = 81%; mp = 198-199 ^{o}C; ^{1}H NMR (400 MHz, $CDCl_3$) δ 8.57 (d, J = 8.4 Hz, 1H), 8.45 (d, J = 7.8 Hz, 3H), 8.06 (d, J = 8.4 Hz, 1H), 8.02 (d, J = 8.4 Hz, 2H), 7.91 (dd, J = 8.0 Hz, J = 0.8 Hz, 1H), 7.79 – 7.48 (m, 4H), 3.64 – 3.38 (t, 8H). ^{13}C NMR (100.61 MHz, $CDCl_3$) δ 161.25, 154.71, 146.36, 137.11, 132.87, 132.23, 131.08, 128.52, 127.79, 126.82, 126.18, 125.94, 125.14, 123.65, 121.86, 121.02, 120.48, 50.79, 47.04. ESI-MS: (m/z) calcd. for $C_{23}H_{20}N_4O_4S$; 448.12, found: 449.22 $(M + H)^+$. Anal. Calcd for $C_{23}H_{20}N_4O_4S$; (%) C 61.59, H 4.49, N 12.49; found: C 61.64, H 4.61, N 12.54.

5.2.32. 1-(4-(4-(phenanthridin-6-yl)piperazin-1-ylsulfonyl)phenyl)ethanone **(7m)**

Appearance: off white solid; yield = 76%; mp = 204-205 ^{o}C; ^{1}H NMR (400 MHz, $CDCl_3$) δ 8.60 (d, *J* = 8.8 Hz, 1H), 8.46 (d, *J* = 8.0 Hz, 2H), 8.40 (d, *J* = 8.2 Hz, 1H), 8.12 (d, *J* = 8.4 Hz, 1H), 8.04 (d, *J* = 8.0 Hz, 2H), 7.88 (dd, *J* = 8.0 Hz, *J* = 1.2 Hz, 1H), 7.81 – 7.44 (m, 4H), 3.64 – 3.38 (t, 8H), 2.72 (s, 3H). ^{13}C NMR (100.61 MHz, $CDCl_3$) δ 171.47, 160.68, 152.23, 145.22, 138.22, 132.46, 132.67, 130.97, 129.42, 128.84, 127.46, 126.17, 124.24, 124.08, 123.68, 121.22, 120.88, 120.56, 50.64, 46.03, 29.44. ESI-MS: (m/z) calcd. for $C_{25}H_{23}N_3O_3S$; 445.14, found: 446.25 $(M + H)^+$. Anal. Calcd for $C_{25}H_{23}N_3O_3S$; (%) C 67.40, H 5.20, N 9.43; found: C 67.49, H 5.24, N 9.47.

5.2.33. 6-(4-(5-bromothiophen-2-ylsulfonyl)piperazin-1-yl)phenanthridine **(7n)**

Appearance: pale yellow solid; yield = 80%; mp = 162-163 ^{o}C; ^{1}H NMR (400 MHz, $CDCl_3$) δ 8.58 (d, *J* = 8.4 Hz, 1H), 8.45 (d, *J* = 7.8 Hz, 1H), 8.08 (d, *J* = 8.2 Hz, 1H), 8.93 (d, *J* = 8.0 Hz, 1H), 7.81 – 7.50 (m, 4H), 7.38 (d, *J* = 7.2 Hz, 1H), 7.16 (d, *J* = 7.4 Hz, 1H), 3.66 – 3.40 (t, 8H). ^{13}C NMR (100.61 MHz, $CDCl_3$) δ 162.24, 151.47, 144.78, 139.41, 134.89, 133.01, 131.22, 128.41, 126.84, 126.12, 125.08, 124.86, 123.25, 123.11, 122.47, 120.78, 119.23, 50.48, 46.14. ESI-MS: (m/z) calcd. For $C_{21}H_{18}BrN_3O_2S_2$; 487.00, found: 487.13 $(M + H)^+$. Anal. Calcd for $C_{21}H_{18}BrN_3O_2S_2$; (%) C 51.64, H 3.71, N 8.60; found: C 51.78, H 3.75, N 8.69.

5.3. Microplate Alamar Blue Assay (MABA)

The anti-mycobacterial activities of title compounds **6a-s** and **7a-n** were evaluated against MTB H37Rv (ATCC 27294) strain using MABA [27,28]. 200µL of sterile deionized water was added to all outer-perimeter wells of sterile 96-well plates to minimize evaporation of the medium in the test wells during incubation. The wells in rows B to G in columns 3 to 11 received 100µl of 7H9GC broth. 100µL of 2× drug solutions were added to the wells in rows B to G in columns 2 and 3. By using a multichannel pipette, 100µl was transferred from column 3 to column 4, and the contents of the wells were mixed well. Identical serial 1:2 dilutions were continued through column 10, and 100µl of excess medium was discarded from the wells in column 10.

100µL of MTB inoculum was added to the wells in rows B to G in columns 2 to 10. Add 100µL of medium to B11 and C11 (media control), 100µL of MTB inoculum to D11 and E11 and 100µL of MTB inoculum with 3-5% DMSO to F11 and G11 (solvent control).

The plates were sealed with parafilm and were incubated at 37°C for 5 days. 50µL of a freshly prepared 1:1 mixture of 10× Alamar Blue (Accumed International, Westlake, Ohio)

reagent and 10% Tween 80 was added to well D11. The plates were reincubated at 37°C for 24 h. If well D11 turned pink, the reagent mixture was added to all wells in the microplate (if the well remained blue, the reagent mixture would be added to another control well and the result would be read on the following day). The microplates were resealed with parafilm and were incubated for an additional 24 h at 37°C, and the colors of all wells were recorded. A blue color in the well was interpreted as no growth, and a pink color was scored as growth. A few wells appeared violet after 24 h of incubation, but they invariably changed to pink after another day of incubation and thus were scored as growth (while the adjacent blue wells remained blue). The MIC was defined as the lowest drug concentration which prevented a color change from blue to pink.

5.4. Molecular modelling studies:

The 2D structures of synthesized compounds (**6a-s** and **7a-n**) were sketched and converted to 3D using Ligprep, module of Schrodinger suite package 2013. ATPase domain of *Mycobacterium tuberculosis* GyrB protein was selected and prepared for docking by protein preparation wizard which was a part of the Maestro software [29]. Bond orders and formal charges were added for hetero groups, and hydrogens were added to all atoms in the system. Water molecules within 5 Å distance were removed. For each structure, a brief relaxation was performed using an all-atom constrained minimization carried out with the Impact Refinement module (Impref). (Impact v5.8, Schro¨dinger, LLC, New York, NY) using the OPLS-2005 force field to alleviate steric clashes that may exist in the original PDB structure. The minimization was terminated when the energy converged or the RMSD reached a maximum cut off of 0.30 Å. The binding site was defined by a rectangular box surrounding the ANP and coordinates of grid box were X = -21.987185, Y=26.604429, Z=-50.838890. Prepared ligands were docked into the ANP binding pocket of MTB GyrB protein with Glide 5.0 (Glide v6.0 Schrodinger, LLC, New York, NY) [30]. Glide energy grids were generated for each of the prepared complexes. Glide XP (Extra Precision) docking with ligand flexibility was performed. A total of ten ligand conformations were allowed and finally top score conformation was selected as active conformation. Molecules were analyzed based on docking score, interacting amino acids and hydrogen bonds.

5.5. Cytotoxicity assay

Most active anti-TB compounds (MIC ≤ 12.5 µg/mL) were further examined for toxicity in RAW 264.7 cell lines at the concentration of 50 µg/mL. After 72 h of exposure, viability was

assessed on the basis of cellular conversion of MTT into a formazan product using the Promega Cell Titer 96 non-radioactive cell proliferation assay [31].

Acknowledgements

The financial assistance provided by Department of Biotechnology, (No.BT/PR4801/MED/29/370/2012), New Delhi, India is gratefully acknowledged.

References:

[1]. World Health Organization (WHO) - Global Tuberculosis Control 2014 report. http://www.who.int/tb/publications/global_report/en/ Geneva, Switzerland, 2014.

[2]. K.K. Ashish, N. Dahiya, Tuberculosis. 94 (2014) 357−362.

[3]. A. Parhi, C. Kelley, M. Kaul, P.S. Daniel, J.L. Edmond, Bioorg. Med. Chem. Lett. 22 (2012) 7080–7083.

[4]. C. Laura, C. Filippo, L. Marco, L. Alessandro De, A. Emanuela, T-D. Yuk-Ching, L. Valentina, S. Claudia, Bioorg. Med. Chem. Lett. 21 (2011) 7041–7044.

[5]. M. Duksi, D. Baretic, V. Caplar, I. Piantanida, Eur. J. Med. Chem. 45 (2010) 2671–2676.

[6]. I. Kock, D. Heber, M. Weide, U. Wolschendorf, B. Clement, J. Med. Chem. 2005, 48, 2772–2777.

[7]. K. Matsumoto, T. Choshi, M. Hourai, Y. Zamami, K. Sasaki, T. Abe, M. Ishikura, N. Hatae, T. Iwamura, S. Tohyama, J. Nobuhiro, S. Hibino, Bioorg. Med. Chem. Lett. 22 (2012) 4762–4764.

[8]. N. W. Luedtke, Q. Liu, Y. Tor, Bioorg. Med. Chem. 11 (2003) 5235–5247.

[9]. A. Hiroshi, S. Kazuyuki, N. Masahiko, A. Atsushi, M.T.A. Salim, O. Mika, B. Masanori, H. Yuichi, Bioorg. Med. Chem. 19 (2011) 2675–2687.

[10]. A.-D. Yapi, N. Desbois, J-M. Chezal, O. Chavignon, J-C. Teulade, A. Valentin, Y. Blache, Eur. J. Med. Chem. 45 (2010) 2854–2859.

[11]. D. Cappoen, P. Claes, J. Jacobs, R. Anthonissen, V. Mathys, L. Verschaeve, K. Huygen, K. Norbert De, J. Med. Chem. 57 (2014**)** 2895–2907.

[12]. H.N. Nagesh, N. Suresh, K. Mahalakshmi Naidu, B. Arun, J.P. Sridevi, D. Sriram, P. Yogeeswari, K.V.G. Chandra Sekhar, Eur. J. Med. Chem. 74 (2014) 333–339.

[13]. H.N. Nagesh, K. Mahalakshmi Naidu, D.H. Rao, J.P. Sridevi, D. Sriram, P. Yogeeswari, K.V.G. Chandra Sekhar, Bioorg. Med. Chem. Lett. 23 (2013) 6805–6810.

[14]. D. Cappoen, J. Jacobs, T.N. Van, S. Claessens, G. Diels, R. Anthonissen, T. Einarsdottir, M. Fauville, L. Verschaeve, K. Huygen, K. Norbert De, Eur. J. Med. Chem. 48 (2012) 57–68.

[15]. T. Ishikawa, Med. Res. Rev. 21 (2001) 61–72.

[16]. P.N. Mortenson, C.W. Murray, J. Comput. Aided. Mol. Des. 25 (2011) 663–667.

[17]. P.K. Ranjith, P. Rajeesh, K.R. Haridas, S.N. Kumari, Eur. J. Med. Chem. 71 (2014) 354–365.

[18]. K. Mahalakshmi Naidu, A. Suresh, J. Subbalakshmi, D. Sriram, P. Yogeeswari, P. Raghavaiah, K.V.G. Chandra Sekhar, Eur. J. Med. Chem. 87 (2014) 71–78.

[19]. N.P. Kavitkumar, N.T. Vikas, Eur. J. Med. Chem. 75 (2014) 43–56.

[20]. P.T. Rajendra, Y. Raghunandan, E.L. Robin, J.M.L. Anne, E.L. Richard, J. Med. Chem. 48 (2005) 8261–8269.

[21]. K.D. Thomas, A.V. Adhikari, I.H. Chowdhury, E. Sumesh, K.P. Nishith, Eur. J. Med. Chem. 46 (2011) 2503–2512.

[22]. A. Punkvang, P. Saparpakorn, S. Hannongbua, P. Wolschann, A. Beyer, P. Pungpo, Eur. J. Med. Chem. 45 (2010) 5585–5593.

[23]. A. Agrawal, M. Roué, C. Spitzfaden, S. Petrella, A. Aubry, M. Hann, B. Bax[2], C. Mayer, Biochem. J. 456 (2013) 263–273.

[24]. R.A. Friesner, R.B. Murphy, M.P. Repasky, L.L. Frye, J.R. Greenwood, T.A. Halgren, P.C. Sanschagrin, D.T. Mainz, J. Med Chem. 49 (2006) 6177–6196.

[25]. A. Kamal, P. Swapna, R.V.C.R.N.C. Shetti, A.B. Shaik, M.P. Narasimha Rao, F. Sultana, I.A. Khan, S. Sharma, N.P. Kalia, S. Kumar, B. Chandrakant, Eur. J. Med. Chem. 64 (2013) 239–251.

[26]. G.M. Sheldrick. SHELX97 Program for Crystallography Refinement; University of Go¨ttingen: Germany, (1997).

[27]. L.A. Collins, S.G. Franzblau, Antimicrob. Agents Chemother. 41 (1997) 1004-1009.

[28]. S.G. Franzblau, R.S. Witzig, J.C. McLaughlin, P. Torres, G. Madico, A. Hernandez, M.T. Degnan, M.B. Cook, V.K. Quenzer, R.M. Ferguson, R.H. Gilman, J. Clin. Microb. 36 (1998) 362–366.

[29]. Maestro, version 9.5, Schrödinger, LLC, New York, NY, 2013.

[30]. Schrödinger Suite 2013 QM-Polarized Ligand Docking protocol; Glide version 6.0, Schrödinger, LLC, New York, NY, 2013; Jaguar version 8.1, Schrödinger, LLC, New York, NY, 2013; QSite version 6.0, Schrödinger, LLC, New York, NY, 2013.

[31]. D. Gerlier, N. Thomasset, Immunol. Methods. 94 (1986) 57–63.

Figure 1: Design strategy to achieve title compounds

Figure 2: Interaction profile of ANP with ATPase domain of *Mycobacterium tuberculosis* GyrB protein. The hydrophobic pocked is highlighted with the residues interacting with the crystal ligand

Figure 3: Interaction profile of compound **6b** with ATPase domain of *Mycobacterium tuberculosis* GyrB protein. The various hydrophobic interactions of compound **6b** are noticeable.

Figure 4: Interaction profile of compound **7d** with ATPase domain of *Mycobacterium tuberculosis* GyrB protein. The different polar contacts, π-π interaction and the hydrophobic interactions with compound **7d** are noticeable

Figure 5: ORTEP plot for the compound **6b** and **7d**. All the non-hydrogen atoms are presented by their 50% probability thermal ellipsoids

Scheme 1: General synthetic procedure for title compounds

Table 1: Optimisation of reaction conditions of **6b**[a]

Table 2: Antimycobacterial activities of compound **6a-s** and **7a-n** against MTB H37Rv

Table 3: IC_{50} (µg/mL) and SI values of active compounds

Table 4: Crystal data and structure refinement details for **6b** and **7d**

Table 1: Optimisation of reaction conditions of **6b**[a]

Entry	Solvent	Base	Reagent	Temperature (^{o}C)	Time	Yield (%)[b]
1	DCM	TEA	EDC.HCl, HOBt	rt	8 h	58
2	DMF	TEA	EDC.HCl, HOBt	rt	8 h	52
3	DMF	DIPEA	HATU	rt	8 h	41
4	DMF	DIPEA	BOP	rt	8 h	42
5	DMF	DIPEA	PyBOP	rt	8 h	38
6	DCM	Pyridine	T_3P	rt	4 h	54
7	DCM	TEA	T_3P	rt	2 h	56
8	DCM	TEA	T_3P	rt	4 h	68
9	DCM	TEA	T_3P	rt	6 h	84
10	DCM	TEA	T_3P	rt	8 h	85
11	DCM	TEA	T_3P	rt	12 h	84

[a]All the reactions were carried out with **5** (1.0 equiv.), base (2.0 equiv.) and reagent (1.0-1.6 equiv.) in solvent,
[b]Isolated yield after column chromatography.

Table 2: Antimycobacterial activities of compounds **6a-s** and **7a-n** against MTB H37Rv

S.No.	Entry	R_1 / R_2	MIC(µg/mL) against MTB H_{37}Rv strain
1	**6a**	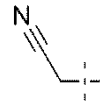	25
2	**6b**	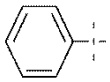	3.13
3	**6c**	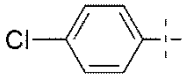	12.5
4	**6d**	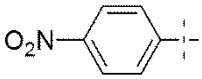	50
5	**6e**	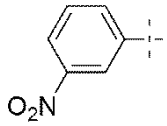	3.13
6	**6f**	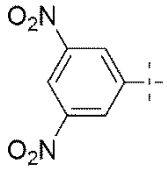	25
7	**6g**	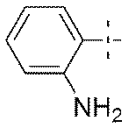	>50
8	**6h**	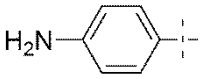	50
9	**6i**	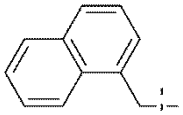	>50
10	**6j**	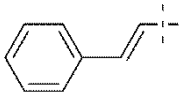	12.5
11	**6k**	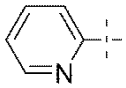	3.13
12	**6l**	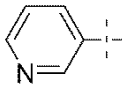	6.25
13	**6m**	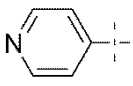	1.56
14	**6n**	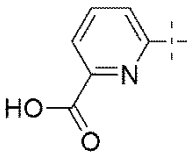	3.13

15	**6o**	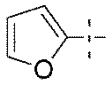	25
16	**6p**	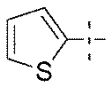	50
17	**6q**	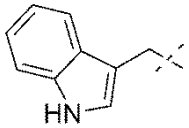	25
18	**6r**	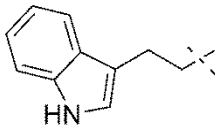	6.25
19	**6s**	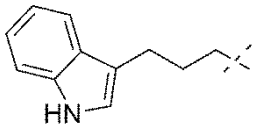	1.56
20	**7a**		25
21	**7b**	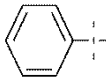	6.25
22	**7c**	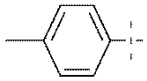	>50
23	**7d**	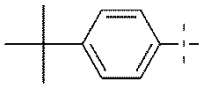	1.56
24	**7e**	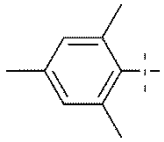	12.5
25	**7f**	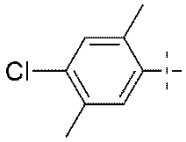	6.25
26	**7g**	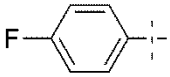	6.25
27	**7h**	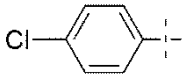	3.13
28	**7i**	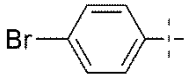	3.13
29	**7j**	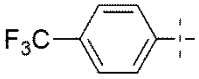	25

30	**7k**	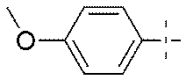	6.25
31	**7l**	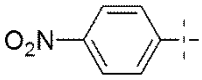	50
32	**7m**	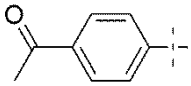	25
33	**7n**	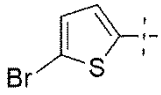	3.13
-	Isoniazid	-	0.1
-	Rifampicin	-	0. 2
-	Pyrazinamide	-	6.25

Table 3: IC_{50} (µg/mL) and SI values of active compounds

Entry	MIC (µg/mL) in MTB H37Rv	% cell inhibition at 50 µg/mL	IC_{50} approximation	[a]SI values
6b	3.13	22.16	112.81	36.15
6c	12.5	26.50	94.33	7.54
6e	3.13	34.64	72.17	23.13
6j	12.5	22.12	113.01	9.04
6k	3.13	42.16	59.29	19.00
6l	6.25	19.16	130.48	20.87
6m	1.56	27.90	89.60	57.43
6n	3.13	26.52	94.26	30.21
6r	6.25	34.64	72.17	11.54
6s	1.56	34.12	73.27	46.96
7b	6.25	30.72	81.38	13.02
7d	1.56	28.92	86.44	55.41
7e	12.5	26.52	94.26	7.54
7f	6.25	34.64	72.17	11.54
7g	6.25	32.76	76.31	12.21
7h	3.13	20.92	119.50	38.30
7i	3.13	28.16	88.77	28.45
7k	6.25	26.52	94.26	15.08
7n	3.13	42.16	59.29	38.01

[a] Selectivity index

Table 4: Crystal data and structure refinement details for **6b** and **7d**

Compound	**6b**	**7d**
Formula	$C_{24}H_{21}N_3O$	$C_{27}H_{29}N_3O_2S$
Sum formula weight	367.44	459.60
Temperature/K	293	293
Crystal system	Triclinic	Monoclinic
Space group	$P\bar{1}$	$P2_1/n$
a (Å)	9.4717 (13)	12.5058(13)
b (Å)	9.6936 (14)	14.6774 (17)
c (Å)	11.8432 (16)	13.3524 (14)
Angle α, β, γ (°)	73.767 (12), 74.207 (12), 65.560 (14)	90, 89.451 (9), 90
Volume ($Å^3$)	935.1 (2)	2450.8(5)
Z	2	4
F(000)	388.0	976.0
D_{calc} (g/mm^3)	1.305	1.246
μ (mm^{-1})	0.081	0.16
Absorption correction:	Multi-scan	Multi-scan
Radiation wavelength (Å)	0.71073	0.71073
Radiation type	MoK_α	MoK_α
Radiation monochromator	Graphite	Graphite
$(h, k, l)_{max}$, $(h, k, l)_{min}$	(12, 13, 14), (−12, −13, −14)	(17, 20, 15), (−9, −16, −18)
2Θ range for data collection	6.6 − 58.2°	6.4 − 58.4°
*T*min, *T*max	0.246, 1.000	0.922, 1.000
No. of measured, independent and observed [I > 2σ(I)] reflections	6305, 5019, 2213	7784, 6663, 3305
R_{int}	0.038	0.018
$(\sin \theta/\lambda)_{max}$ ($Å^{-1}$)	0.684	0.687
Crystal size/mm^3	0.6 × 0.5 × 0.4	0.6 × 0.5 × 0.4
$R[F^2 > 2\sigma(F^2)]$, $wR(F^2)$, *S*	0.0757 (2213), 0.2206 (4075), 0.95	0.050 (3305), 0.121 (5149), 1.02
No. of parameters	253	298
$\Delta\rho_{max}$, $\Delta\rho_{min}$ (e $Å^{-3}$)	0.27, −0.28	0.14, −0.25
Structure refinement	SHELXL97 (Sheldrick, 2008)	

Figure 1: Design strategy to achieve title compounds

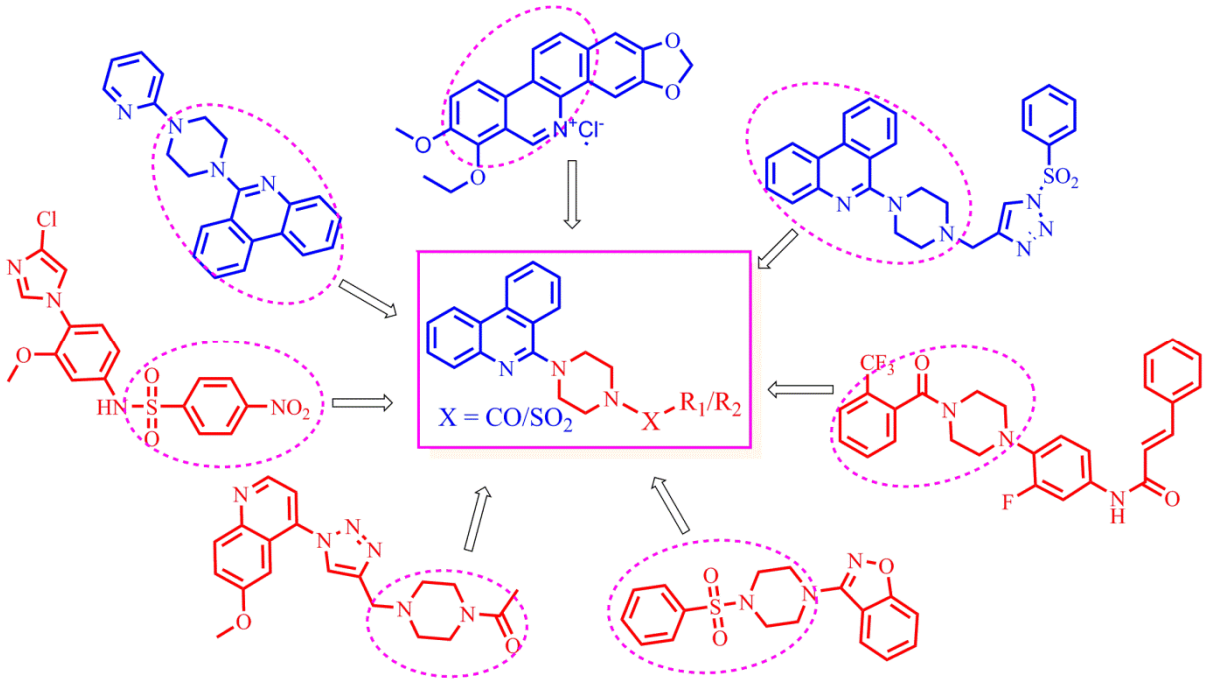

Scheme 1: General synthetic procedure to attain title compounds

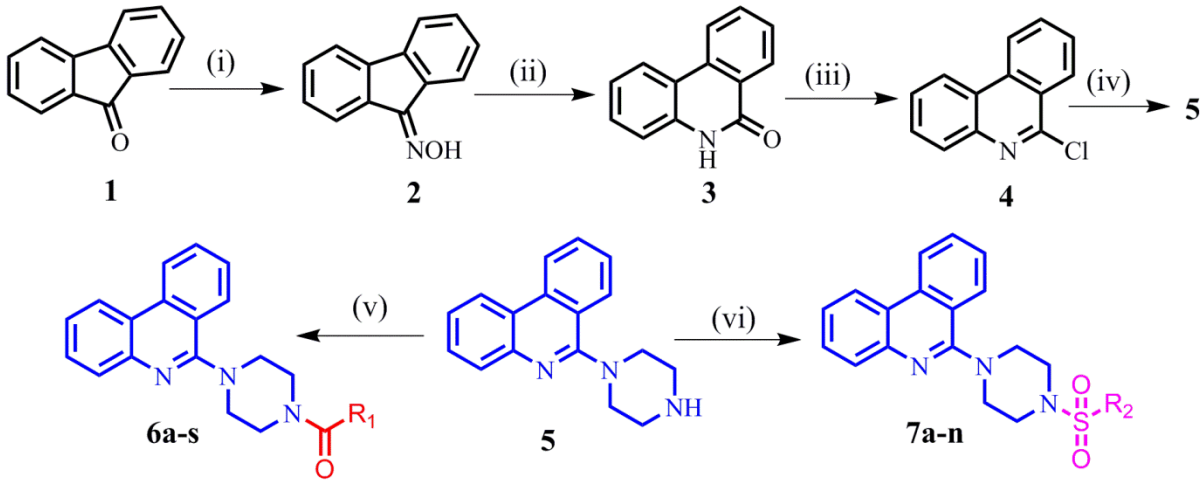

Reagents and conditions: (i) $NH_2OH.HCl$ (1.2 equiv), NaOAc (1.2 equiv), EtOH:H_2O (2:1), rt 2 h (ii) PPA (8.0 equiv), P_2O_5 (0.5 equiv), heating at 150 ^oC, 1 h (iii) $POCl_3$ (6.0 equiv), *N*,*N*-dimethylaniline (0.5 equiv), reflux 4h (iv) piperazine (8.0 equiv), Et_3N (2.0 equiv), DMF, MW, 700 Watt, 15 Min (v) substituted alkyl/aryl acids (1.05 equiv), T_3P (1.2 equiv), Et_3N (2.0 equiv), CH_2Cl_2, rt, 6–8 h (vi) substituted alkyl/aryl sulfonyl chlorides (1.1 equiv), Et_3N (1.2 equiv), CH_2Cl_2, rt, 1–2 h.

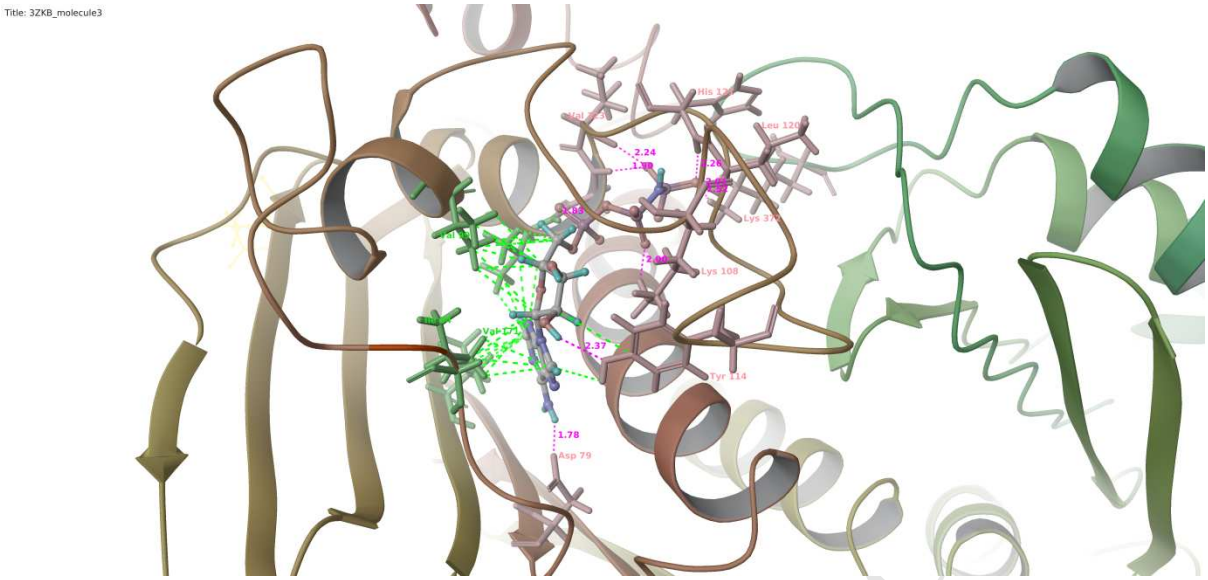

Figure 2: Interaction profile of ANP with ATPase domain of *Mycobacterium tuberculosis* GyrB protein. The hydrophobic pocked is highlighted with the residues interacting with the crystal ligand.

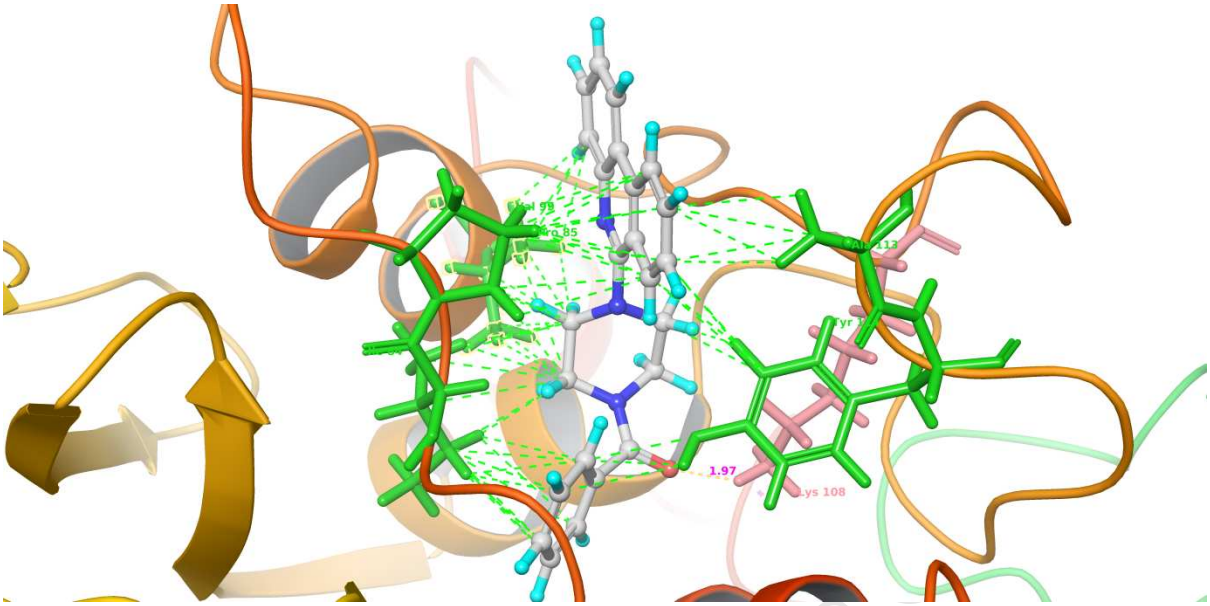

Figure 3: Interaction profile of compound **6b** with ATPase domain of *Mycobacterium tuberculosis* GyrB protein. The various hydrophobic interactions of compound **6b** are noticeable.

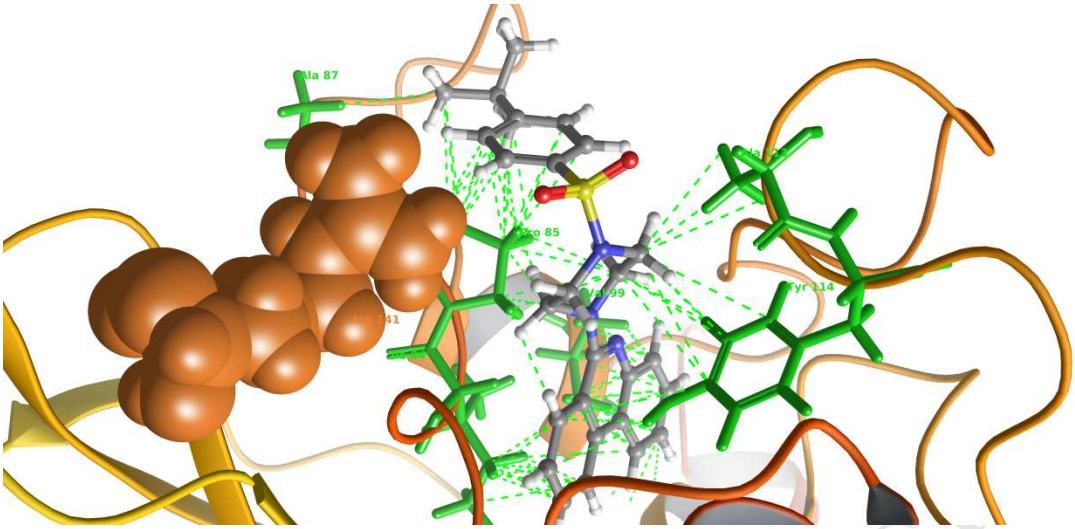

Figure 4: Interaction profile of compound **7d** with ATPase domain of *Mycobacterium tuberculosis* GyrB protein. The different polar contacts, π-π interaction and the hydrophobic interactions with compound **7d** are noticeable.

Figure 5: ORTEP plot for the compound **6b** and **7d**. All the non-hydrogen atoms are presented by their 50% probability thermal ellipsoids.

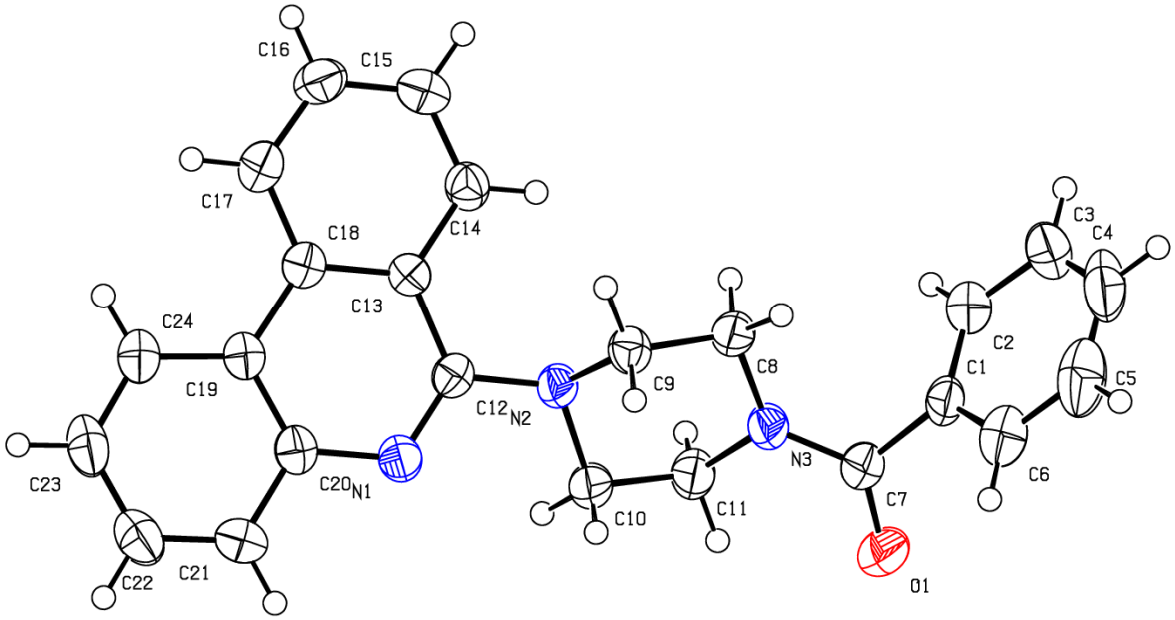

Compound **6b** ORTEP diagram

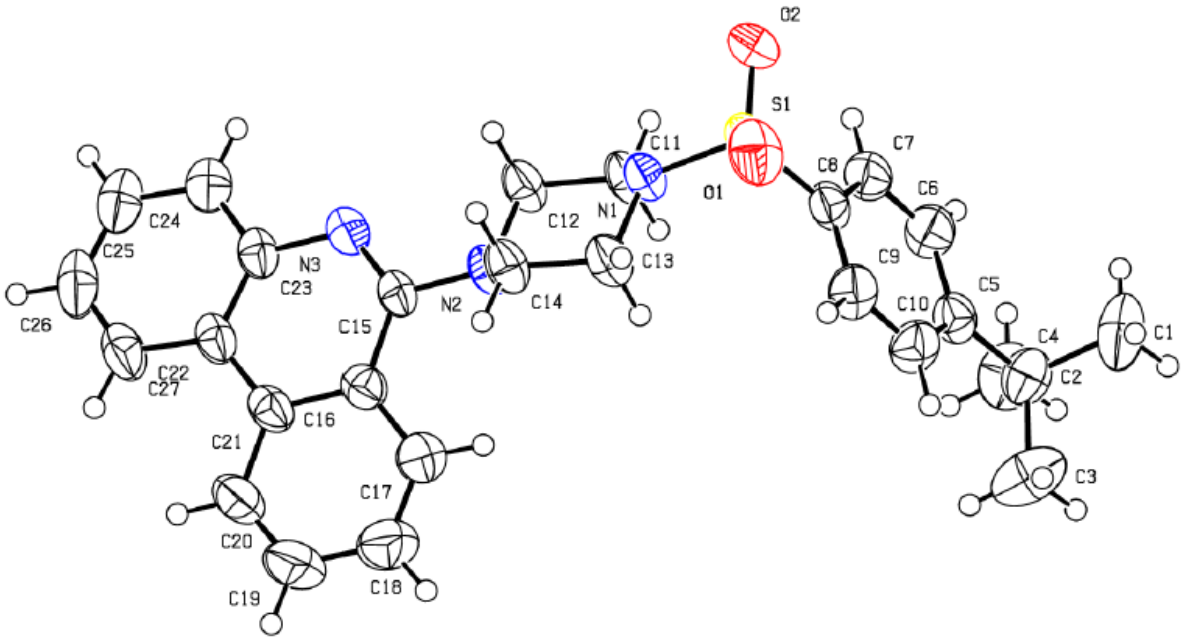

Compound **7d** ORTEP diagram

- ⇨ 33 novel phenanthridines were synthesized and evaluated for anti-TB activity.
- ⇨ 9 analogues (MIC≤3.13) exhibited excellent anti-TB activity against MTB $H_{37}R_{V.}$
- ⇨ *In vitro* toxicity studies were accomplished for most active compounds.
- ⇨ **6b** and **7d** compounds were further substantiated by single crystal X-ray studies.
- ⇨ Compounds **6b** and **7d** were docked to ATPase domain of MTB GyrB protein.

Supplementary Data

Novel 6-(piperazin-1-yl)phenanthridine amide and sulphonamide derivatives as potent *Mycobacterium tuberculosis* H37Rv inhibitors

Kalaga Mahalakshmi Naidu,[a] Hunsur Nagendra Nagesh,[a] Manjeet Singh,[b] Dharmarajan Sriram,[c] Perumal Yogeeswari,[c] Kondapalli Venkata Gowri Chandra Sekhar[a*]

[a]*Department of Chemistry, Birla Institute of Technology & Science-Pilani, Hyderabad campus, Jawahar Nagar, Shamirpet Mandal, Hyderabad-500 078, India.*
[b]*Department of Chemistry, Banaras Hindu University, Varanasi- 221 005, India.*
[c]*Department of Pharmacy, Birla Institute of Technology & Science-Pilani, Hyderabad campus, Jawahar Nagar, Shamirpet Mandal, Hyderabad-500 078, India.*

***Corresponding author:**

K.V.G. Chandra Sekhar, Department of Chemistry,
Birla Institute of Technology and Science-Pilani, Hyderabad campus, Hyderabad-500078, India.
Phone: +91-40-66303527; E-mail address: kvgc@hyderabad.bits-pilani.ac.in, kvgcs@yahoo.com

Contents: Page

1. Spectras

1.1. ^{1}H and ^{13}C NMR spectra's of represented final compounds

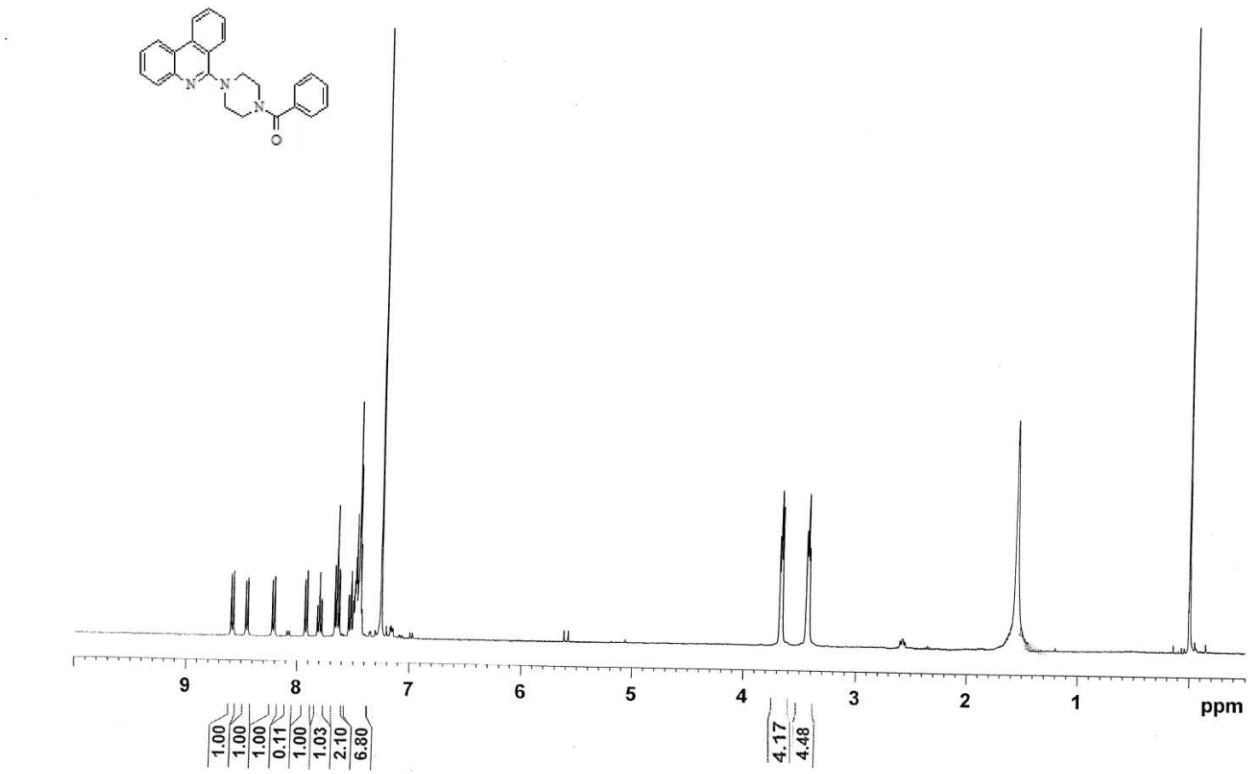

6b ^{1}H NMR

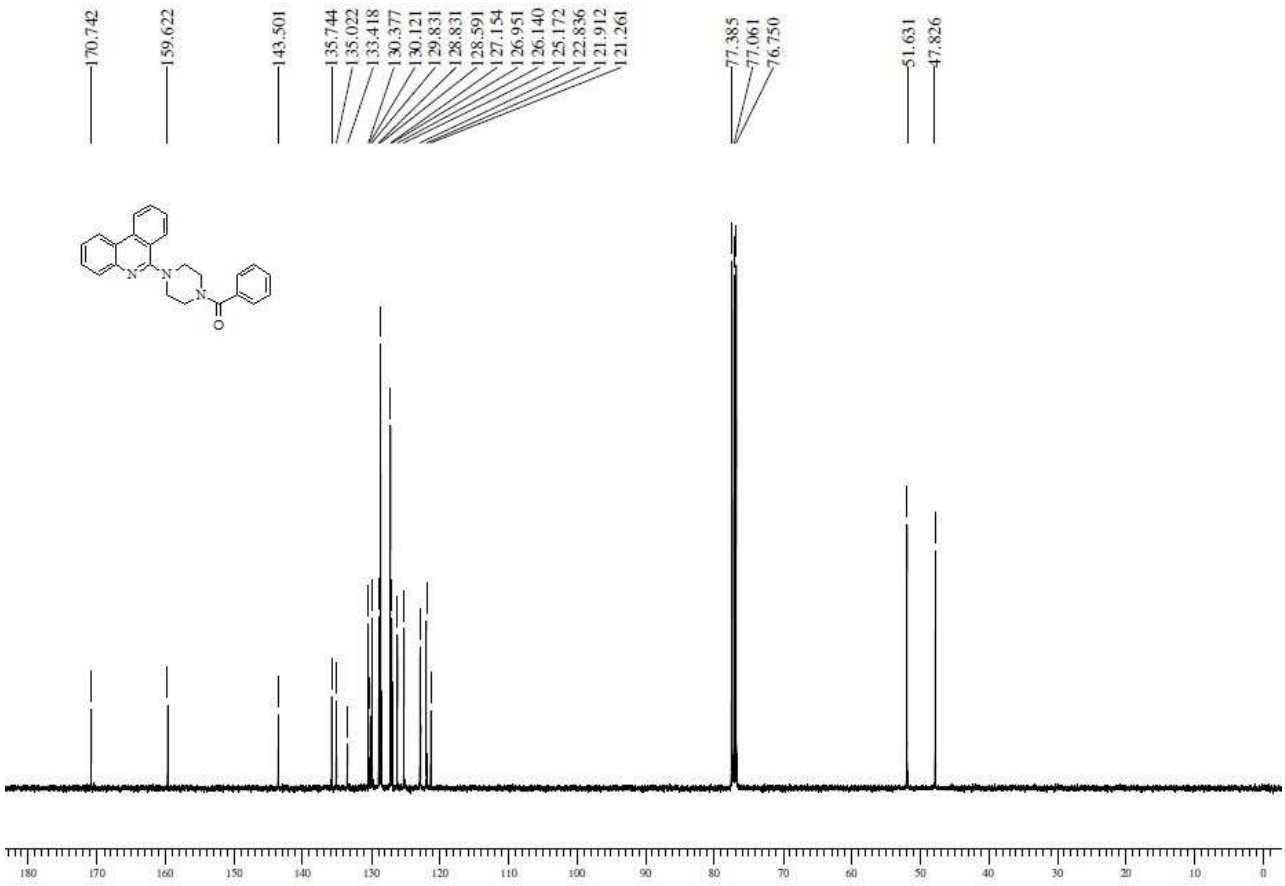

6b ^{13}C NMR

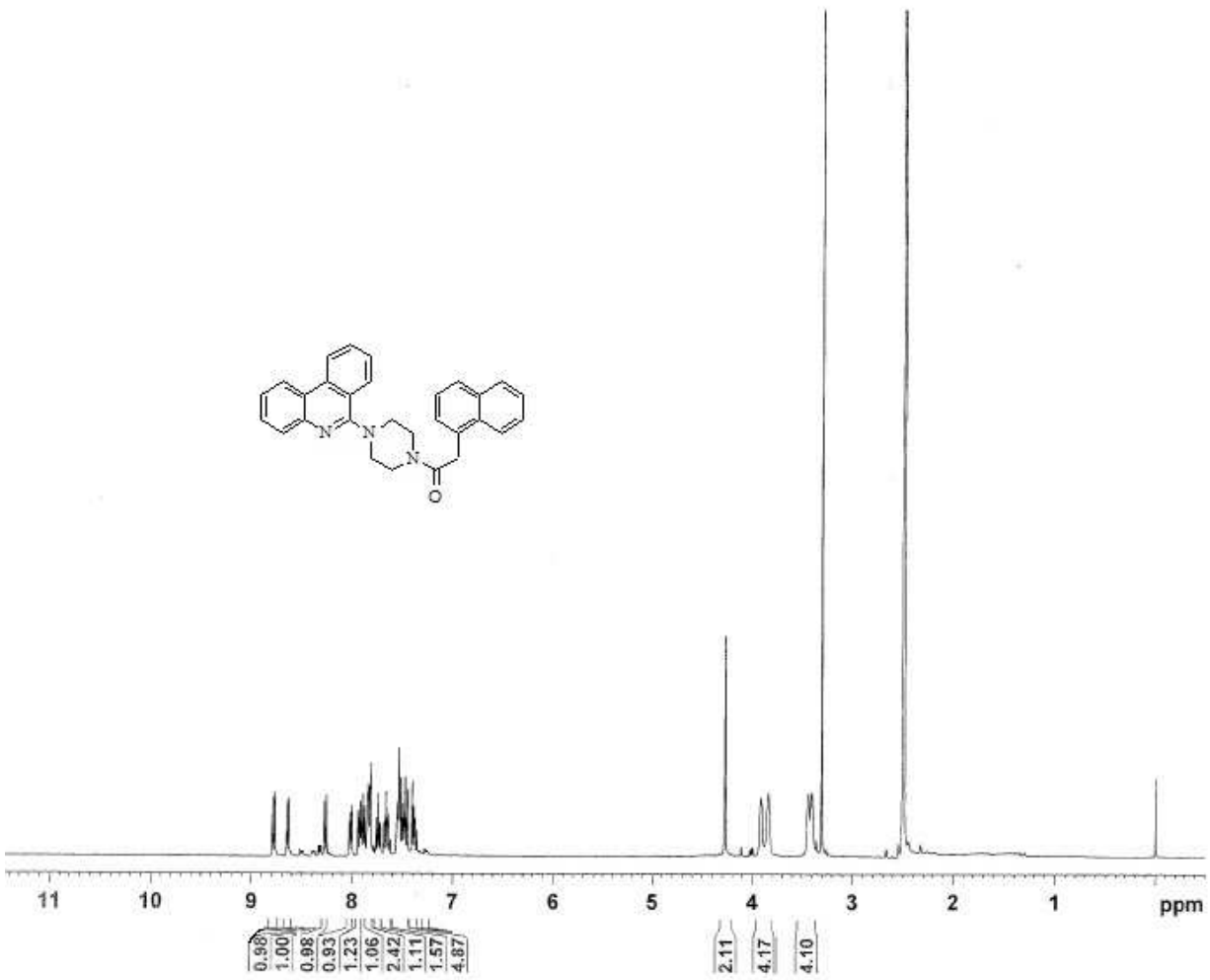

6i ^{1}H NMR

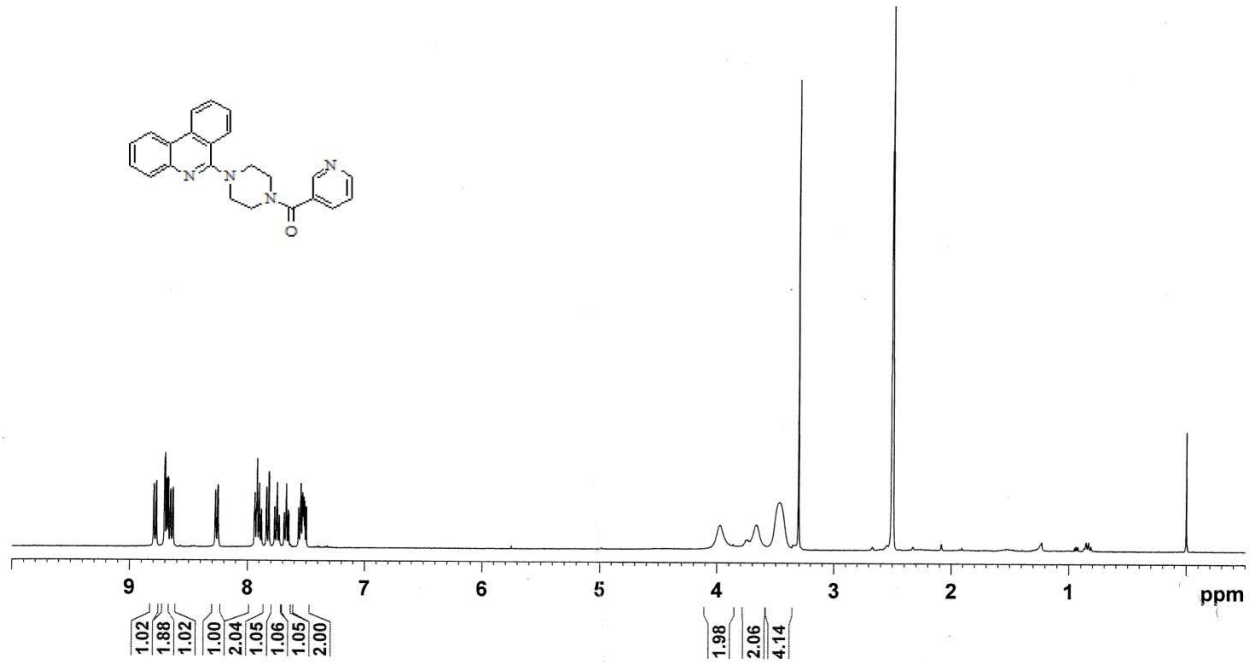

6l ^{1}H NMR

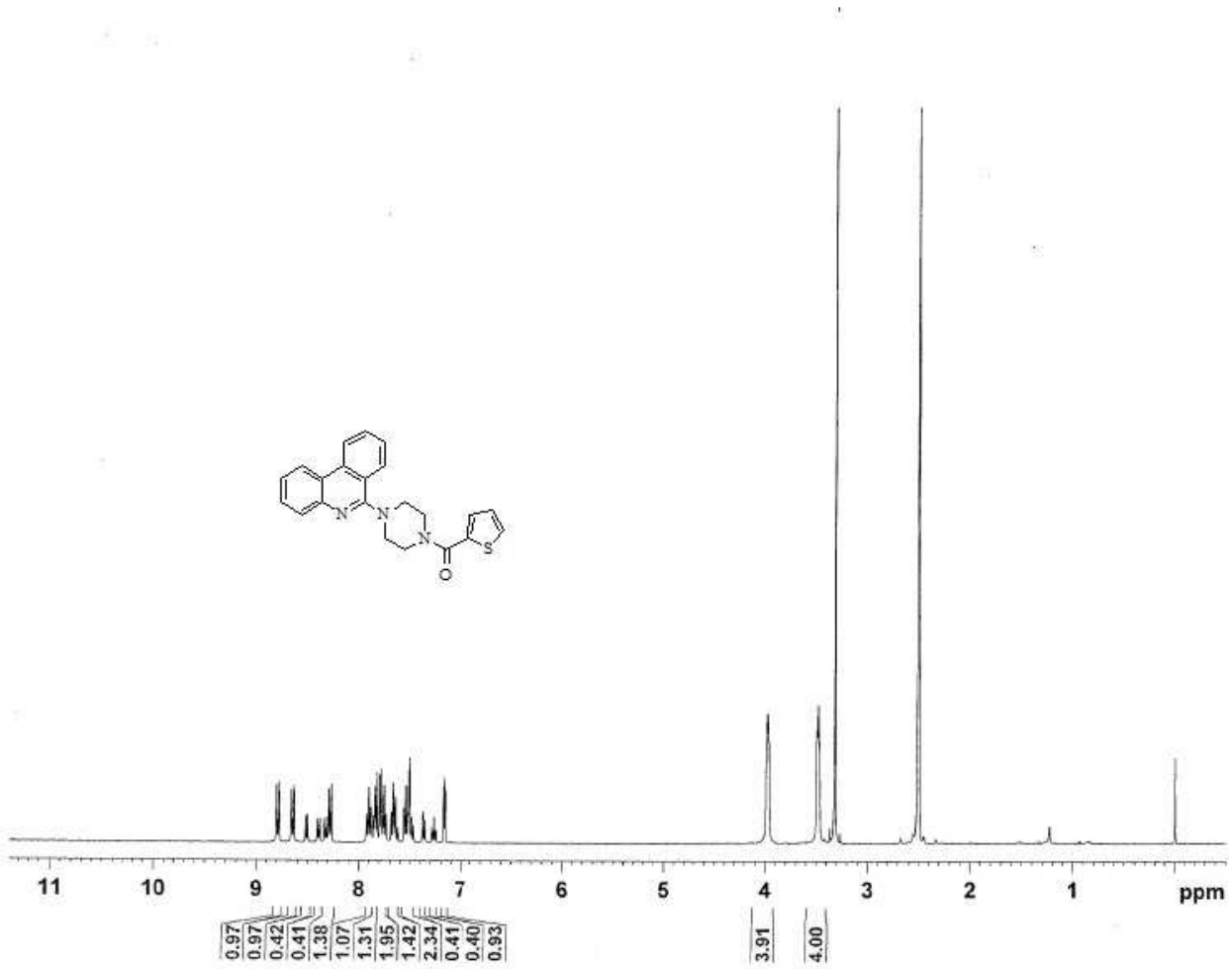

6p ^{1}H NMR

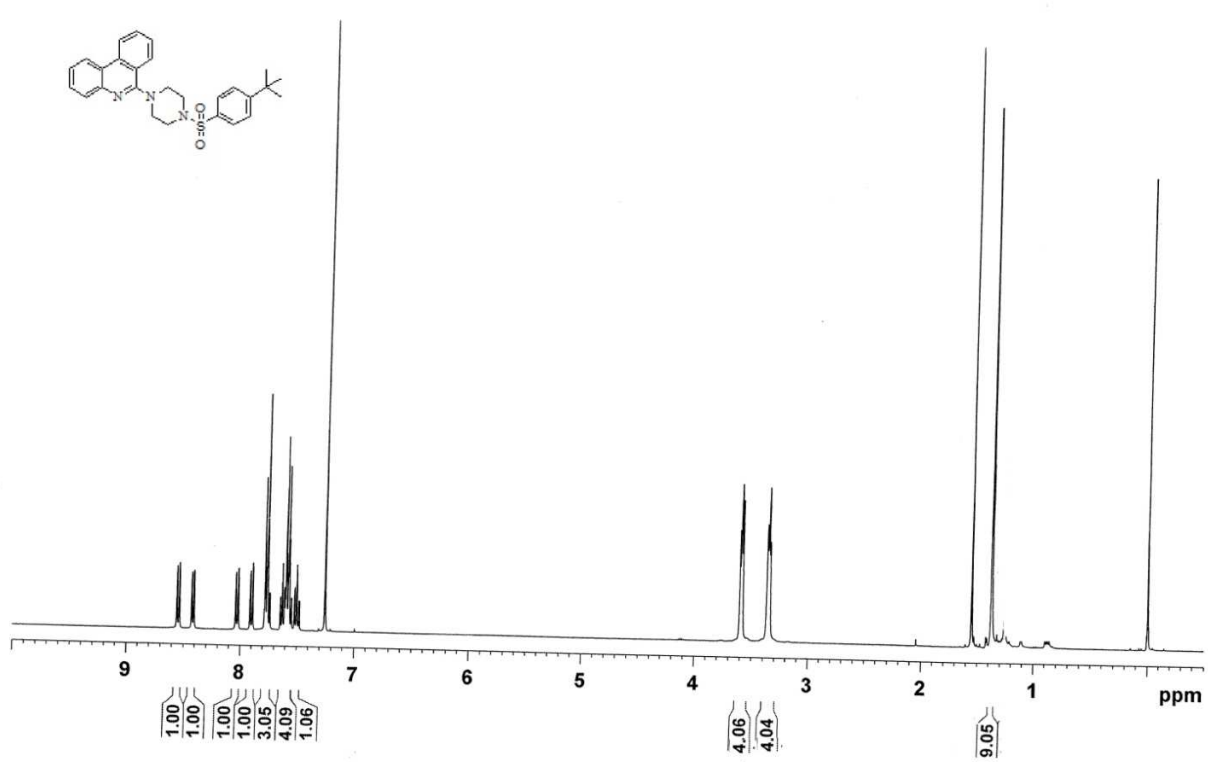

7d ^{1}H NMR

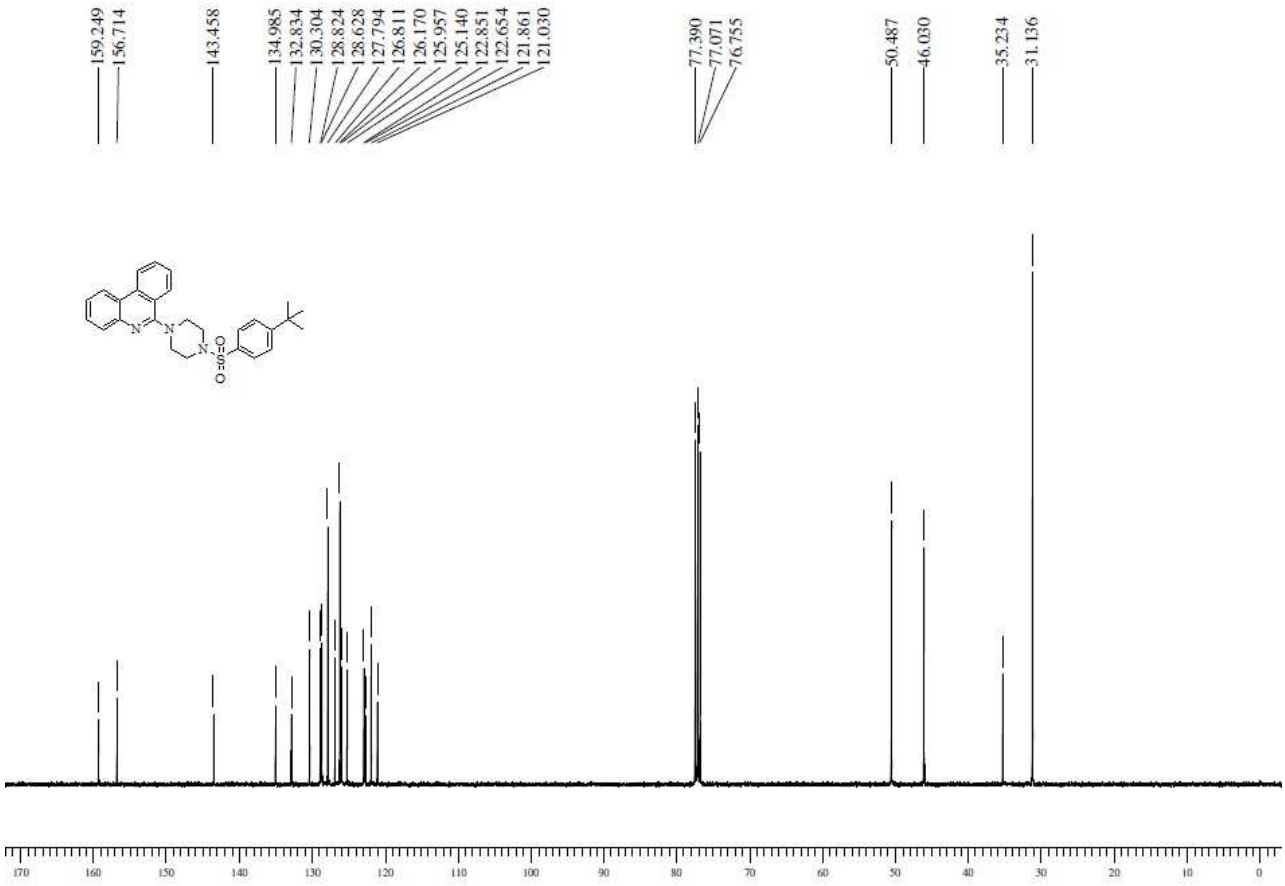

7d ^{13}C NMR

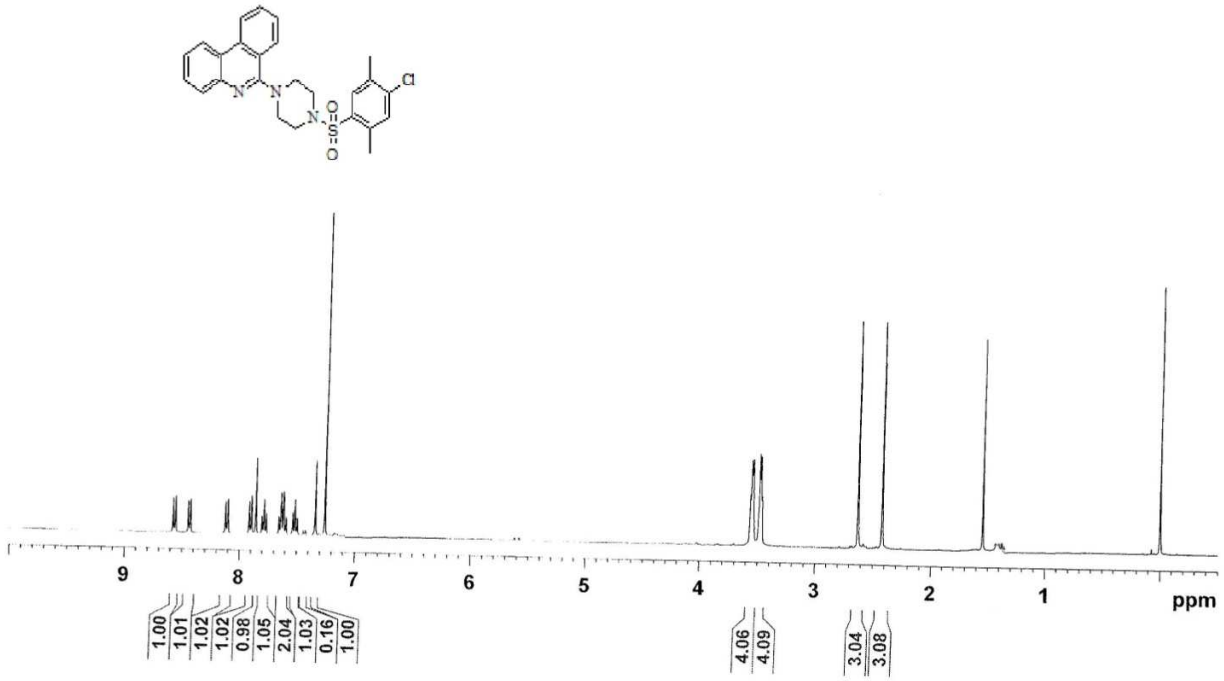

7f ^{1}H NMR

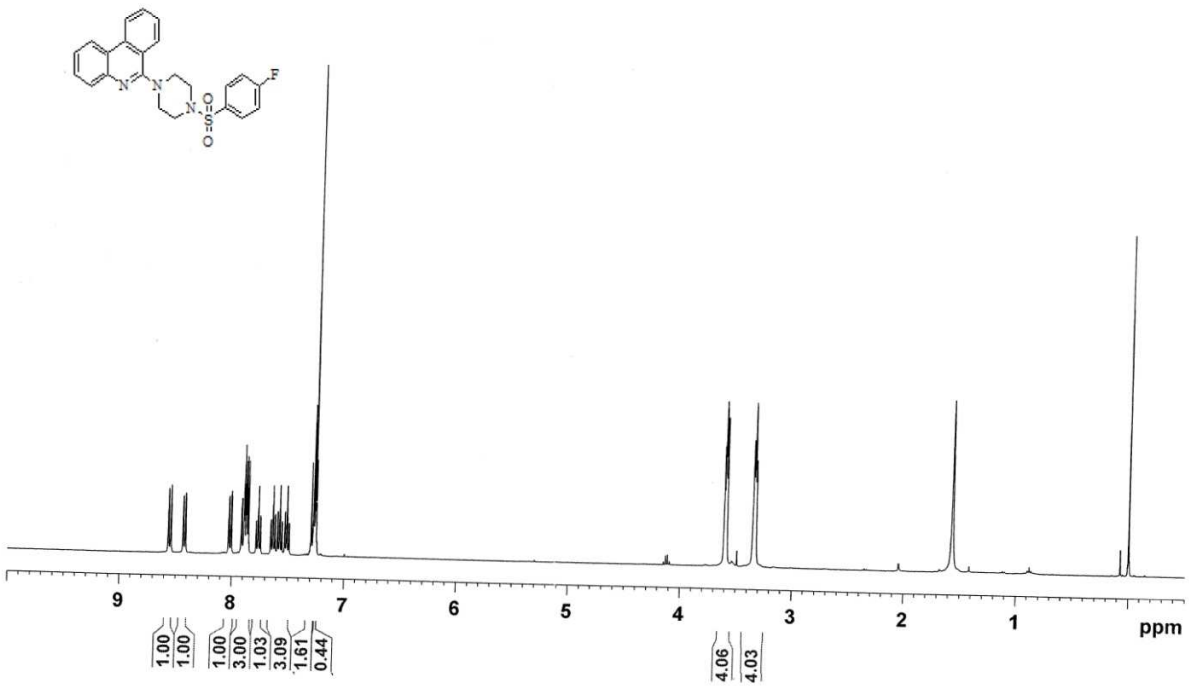

7g ^{1}H NMR

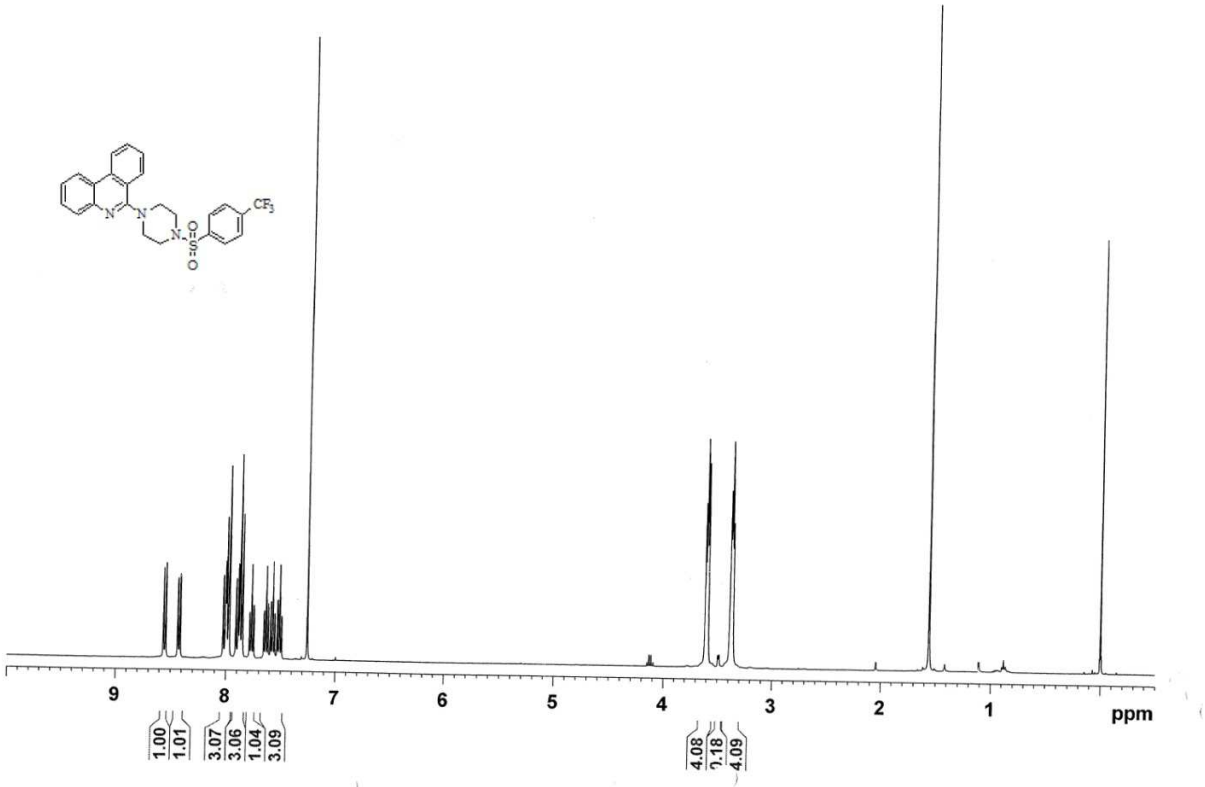

7j ^{1}H NMR

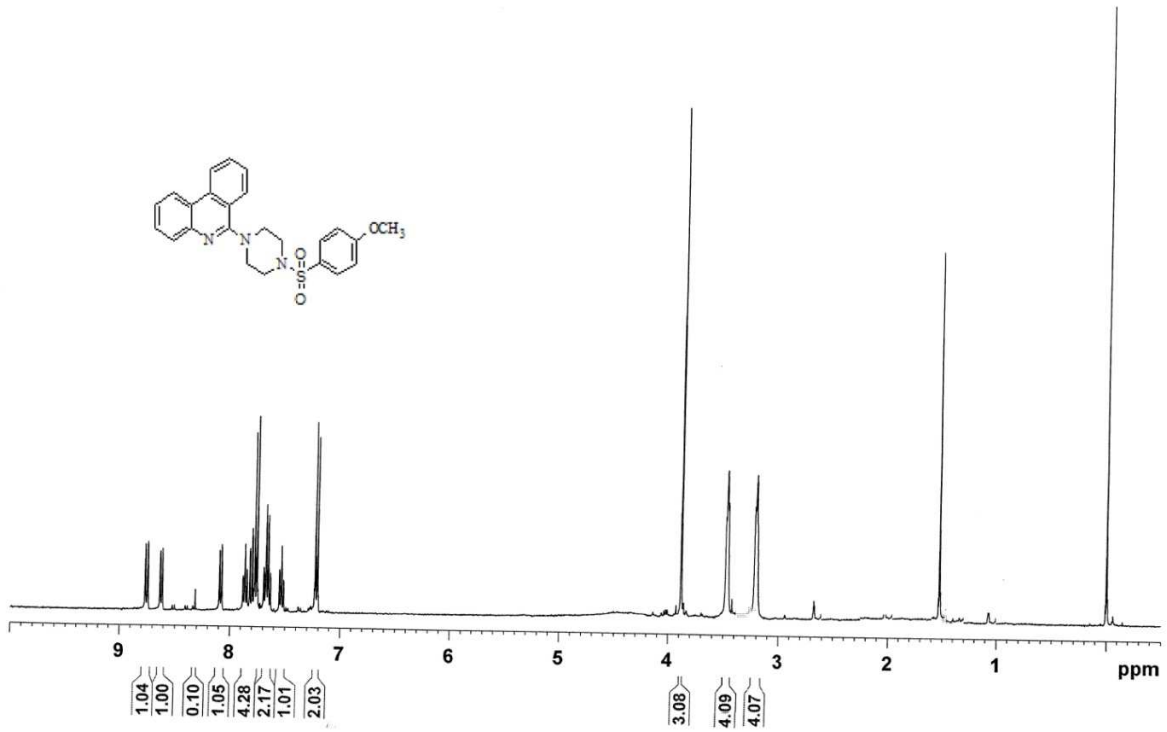

7k ^{1}H NMR

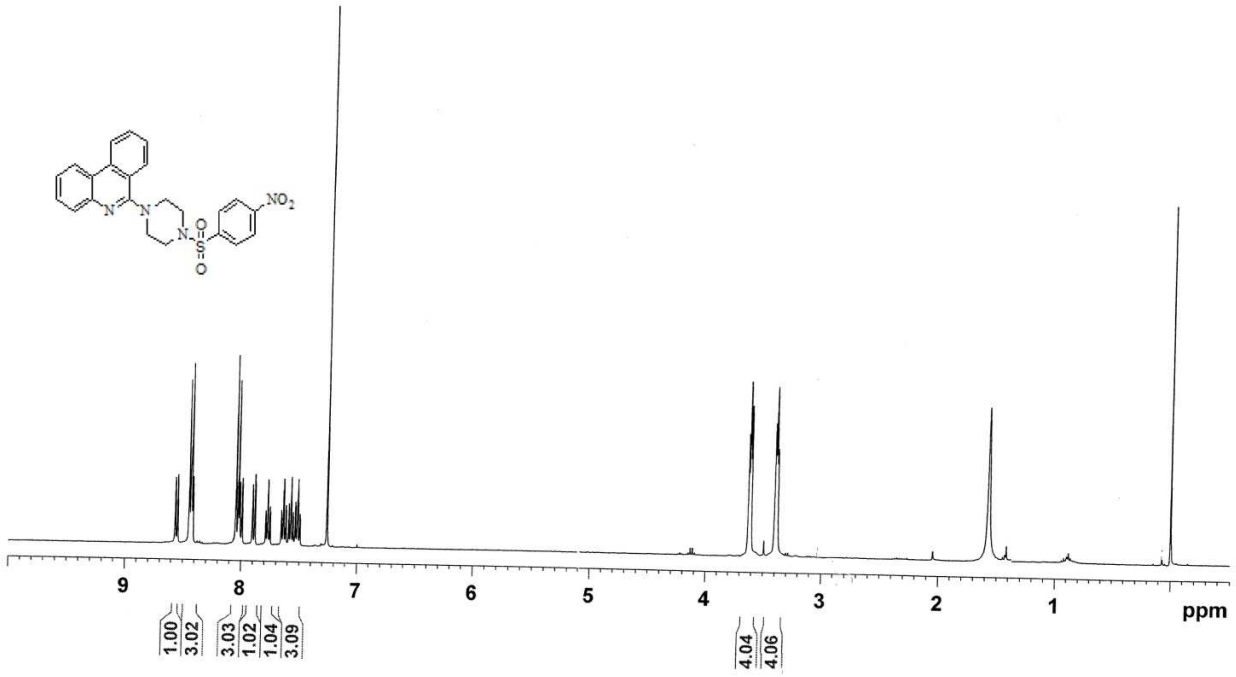

7l ^{1}H NMR

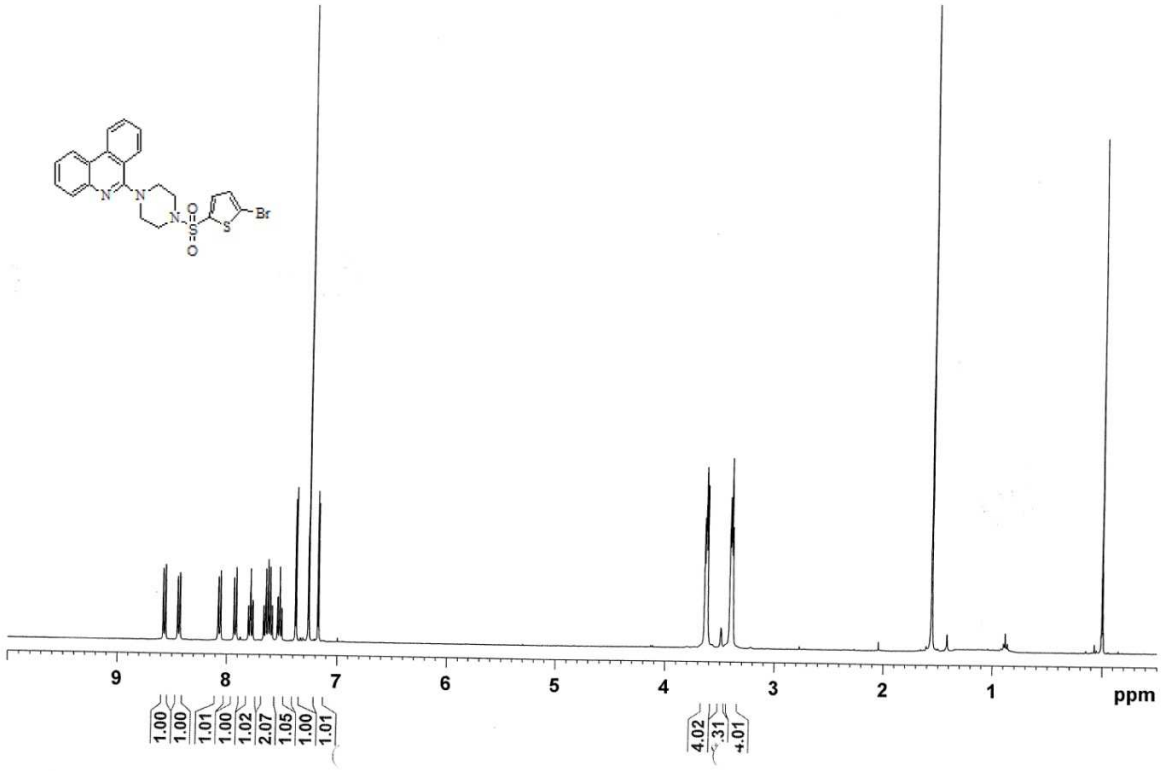

7n ^{1}H NMR

*2. Crystal refinement details and tables 1S-10S: Full list of atomic coordinates thermal parameters, bond distances and angles of **6a** and **7d** crystal structures*

Computing details

Program(s) used to refine structure: *SHELXL97* (Sheldrick, 2008).

*Crystal data for **6b***

CHNO
M_r = 367.44
Triclinic, $P\overline{1}$

a = 9.4717 (13) Å

b = 9.6936 (14) Å
c = 11.8432 (16) A
α = 73.767 (12)°
β = 74.207 (12)°
γ = 65.560 (14)°
V = 935.1 (2) Å^3

Z = 2
F(000) = 388
D_x = 1.305 Mg m^{-3}
Mo $K\alpha$ radiation, λ = 0.71073 Å
Cell parameters from 571 reflections
θ = 3.3–29.3°
μ = 0.08 mm^{-1}
T = 293 K
, white
0.6 × 0.5 × 0.4 mm

Data collection

Radiation source: fine-focus sealed tube
Graphite monochromator
Absorption correction: multi-scan
?
T_{min} = 0.246, T_{max} = 1.000
6305 measured reflections
5019 independent reflections
2213 reflections with $I > 2\sigma(I)$
R_{int} = 0.038
θ_{max} = 29.1°, θ_{min} = 3.3°
h = −12→12
k = −13→13
l = −14→14

Refinement

Refinement on F^2
Least-squares
matrix: full $R[F^2 > 2\sigma(F^2)]$ = 0.076
$wR(F^2)$ = 0.221
S = 0.95
4075 reflections
253 parameters
0 restraints
Primary atom site location: structure-
invariant direct methods
Secondary atom site location:
difference Fourier map Hydrogen site
location: inferred from neighbouring
sites
H atoms treated by a mixture of
independent and constrained
refinement
$w = 1/[\sigma^2(F_o^2) + (0.1054P)^2]$ where
$P = (F_o^2 + 2F_c^2)/3$
$(\Delta/\sigma)_{max}$ = 0.047
$\Delta\rho_{max}$ = 0.27 e Å^{-3}
$\Delta\rho_{min}$ = 0.28 e Å^{-3}

Special details

Geometry. All s.u.'s (except the s.u. in the dihedral angle between two l.s. planes) are estimated using the full covariance matrix. The cell s.u.'s are taken into account individually in the estimation of s.u.'s in distances, angles and torsion angles; correlations between s.u.'s in cell parameters are only used when they are defined by crystal symmetry. An approximate (isotropic) treatment of cell s.u.'s is used for estimating s.u.'s involving l.s. planes.
Refinement. Refinement of F^2 against ALL reflections. The weighted R-factor wR and goodness of fit S are based on F^2, conventional R-factors R are based on F, with F set to zero for negative F^2. The threshold expression of $F^2 > 2\sigma(F^2)$ is used only for calculating R-factors(gt) etc. and is not relevant to the choice of reflections for refinement. R-factors based on F^2 are statistically about twice as large as those based on F, and R- factors based on ALL data will be even larger.

Table 1S: Fractional Atomic Coordinates ($\times 10^4$) and Equivalent Isotropic Displacement Parameters ($Å^2 \times 10^3$) for 6b. U_{eq} is defined as 1/3 of of the trace of the orthogonalised U_{IJ} tensor.

Atom	*x*	*y*	*z*	U_{iso}*/U_{eq}
C2	0.0324 (3)	1.0737 (3)	0.1190 (2)	0.0545 (8)
H2	−0.0145	1.0010	0.1364	0.065*
C3	−0.0592 (4)	1.2241 (4)	0.1328 (3)	0.0705 (11)
H3	−0.1674	1.2527	0.1591	0.085*
N1	0.5774 (2)	0.2605 (2)	0.39124 (18)	0.0385 (5)
C13	0.3312 (3)	0.3338 (3)	0.5330 (2)	0.0311 (6)
C18	0.3902 (3)	0.2004 (3)	0.6187 (2)	0.0326 (6)
C19	0.5486 (3)	0.0918 (3)	0.5881 (2)	0.0327 (6)
C12	0.4338 (3)	0.3564 (3)	0.4190 (2)	0.0320 (6)
N2	0.3716 (2)	0.4846 (2)	0.33013 (17)	0.0356 (5)
C20	0.6364 (3)	0.1286 (3)	0.4749 (2)	0.0356 (6)
C17	0.2917 (3)	0.1777 (3)	0.7303 (2)	0.0432 (7)
H17	0.3289	0.0900	0.7874	0.052*
C14	0.1745 (3)	0.4354 (3)	0.5595 (2)	0.0392 (6)
H14	0.1326	0.5204	0.5019	0.047*
C24	0.6195 (3)	−0.0452 (3)	0.6650 (2)	0.0443 (7)
H24	0.5624	−0.0723	0.7393	0.053*
C15	0.0826 (3)	0.4109 (3)	0.6691 (2)	0.0467 (7)
H15	−0.0200	0.4803	0.6856	0.056*
N3	0.2904 (2)	0.7503 (2)	0.14794 (18)	0.0405 (6)
C16	0.1418 (3)	0.2834 (3)	0.7555 (2)	0.0473 (7)
H16	0.0802	0.2693	0.8305	0.057*
C8	0.2291 (3)	0.7624 (3)	0.2738 (2)	0.0392 (6)
H8A	0.1270	0.7521	0.2974	0.047*
H8B	0.2155	0.8631	0.2844	0.047*
C9	0.3407 (3)	0.6385 (3)	0.3514 (2)	0.0363 (6)
H9A	0.4391	0.6554	0.3337	0.044*
H9B	0.2954	0.6433	0.4348	0.044*
O1	0.3656 (2)	0.8506 (2)	−0.04484 (17)	0.0617 (7)
C21	0.7934 (3)	0.0290 (3)	0.4435 (2)	0.0469 (7)
H21	0.8522	0.0525	0.3690	0.056*
C7	0.2915 (3)	0.8695 (3)	0.0563 (2)	0.0399 (6)
C23	0.7720 (4)	−0.1397 (3)	0.6319 (3)	0.0524 (8)
H23	0.8175	−0.2303	0.6839	0.063*
C10	0.4540 (3)	0.4759 (3)	0.2071 (2)	0.0474 (8)
H10A	0.4826	0.3734	0.1922	0.057*

H10B	0.5497	0.4966	0.1936	0.057*
C1	0.1948 (3)	1.0307 (3)	0.0790 (2)	0.0406 (7)
C6	0.2621 (4)	1.1407 (3)	0.0510 (2)	0.0537 (8)
H6	0.3697	1.1140	0.0216	0.064*
C22	0.8589 (3)	−0.1015 (3)	0.5220 (3)	0.0536 (8)
H22	0.9631	−0.1655	0.5014	0.064*
C11	0.3458 (3)	0.5941 (3)	0.1243 (2)	0.0471 (8)
H11A	0.4011	0.5930	0.0423	0.057*
H11B	0.2555	0.5662	0.1332	0.057*
C4	0.0112 (5)	1.3314 (4)	0.1072 (3)	0.0765 (12)
H4	−0.0496	1.4323	0.1174	0.092*
C5	0.1710 (5)	1.2896 (4)	0.0666 (3)	0.0730 (10)
H5	0.2177	1.3624	0.0495	0.088*

Table 2S: Anisotropic Displacement Parameters ($Å^2 \times 10^3$) for 6a. The Anisotropic displacement factor exponent takes the form: $-2\pi^2[h^2a^{*2}U_{11}+...+2hka\times b\times U_{12}]$

Atom	U^{11}	U^{22}	U^{33}	U^{12}	U^{13}	U^{23}
C2	0.0522 (17)	0.0420 (16)	0.0530 (18)	−0.0105 (15)	−0.0063 (14)	0.0020 (13)
C3	0.069 (2)	0.0491 (19)	0.057 (2)	0.0063 (18)	−0.0096 (16)	−0.0003 (16)
N1	0.0366 (11)	0.0350 (11)	0.0412 (13)	−0.0118 (10)	−0.0078 (9)	−0.0046 (9)
C13	0.0303 (12)	0.0322 (13)	0.0328 (13)	−0.0114 (11)	−0.0075 (10)	−0.0073 (10)
C18	0.0360 (13)	0.0328 (13)	0.0364 (14)	−0.0179 (11)	−0.0092 (10)	−0.0068 (10)
C19	0.0382 (13)	0.0300 (12)	0.0348 (14)	−0.0130 (11)	−0.0123 (10)	−0.0073 (10)
C12	0.0368 (13)	0.0311 (12)	0.0326 (13)	−0.0166 (11)	−0.0069 (10)	−0.0056 (10)
N2	0.0426 (12)	0.0290 (11)	0.0309 (11)	−0.0098 (9)	−0.0050 (9)	−0.0056 (8)
C20	0.0379 (13)	0.0318 (13)	0.0410 (15)	−0.0143 (11)	−0.0122 (11)	−0.0057 (11)
C17	0.0479 (16)	0.0424 (15)	0.0391 (15)	−0.0194 (14)	−0.0104 (12)	−0.0005 (12)
C14	0.0356 (13)	0.0373 (14)	0.0434 (15)	−0.0125 (12)	−0.0109 (11)	−0.0035 (12)
C24	0.0496 (16)	0.0355 (14)	0.0444 (16)	−0.0127 (13)	−0.0149 (12)	−0.0007 (12)
C15	0.0367 (14)	0.0489 (16)	0.0503 (17)	−0.0114 (13)	−0.0018 (12)	−0.0155 (13)
N3	0.0492 (13)	0.0299 (11)	0.0327 (12)	−0.0061 (10)	−0.0055 (9)	−0.0060 (9)
C16	0.0444 (15)	0.0550 (17)	0.0400 (15)	−0.0221 (14)	0.0005 (12)	−0.0071 (13)
C8	0.0481 (15)	0.0326 (13)	0.0324 (14)	−0.0121 (12)	−0.0034 (11)	−0.0070 (11)
C9	0.0424 (14)	0.0305 (13)	0.0383 (14)	−0.0137 (12)	−0.0090 (11)	−0.0076 (11)
O1	0.0743 (15)	0.0511 (12)	0.0396 (12)	−0.0167 (11)	0.0076 (10)	−0.0052 (9)
C21	0.0376 (14)	0.0486 (16)	0.0481 (17)	−0.0108 (14)	−0.0008 (12)	−0.0137 (13)
C7	0.0428 (14)	0.0383 (14)	0.0350 (14)	−0.0134 (12)	−0.0080 (11)	−0.0028 (11)
C23	0.0630 (19)	0.0341 (14)	0.0536 (18)	−0.0050 (14)	−0.0262 (14)	−0.0031 (13)
C10	0.0562 (17)	0.0364 (14)	0.0330 (15)	−0.0061 (13)	−0.0008 (12)	−0.0057 (12)
C1	0.0504 (15)	0.0323 (13)	0.0317 (14)	−0.0110 (13)	−0.0106 (11)	0.0017 (11)
C6	0.0674 (19)	0.0451 (17)	0.0511 (18)	−0.0244 (15)	−0.0182 (14)	0.0005 (14)
C22	0.0466 (16)	0.0442 (16)	0.061 (2)	−0.0023 (14)	−0.0171 (14)	−0.0117 (15)
C11	0.0652 (18)	0.0333 (14)	0.0328 (14)	−0.0092 (13)	−0.0063 (12)	−0.0075 (11)
C4	0.120 (3)	0.0337 (17)	0.053 (2)	0.000 (2)	−0.030 (2)	−0.0027 (15)
C5	0.116 (3)	0.0432 (19)	0.068 (2)	−0.032 (2)	−0.038 (2)	0.0020 (16)

Table 3S: Bond Lengths for **6b**

Atom—Atom	Length/Å	Atom—Atom	Length/Å
C2—C3	1.383 (4)	N3—C8	1.464 (3)
C2—C1	1.395 (4)	N3—C11	1.465 (3)
C2—H2	0.9300	C16—H16	0.9300
C3—C4	1.381 (5)	C8—C9	1.505 (3)

C3—H3	0.9300	C8—H8A	0.9700
N1—C12	1.305 (3)	C8—H8B	0.9700
N1—C20	1.389 (3)	C9—H9A	0.9700
C13—C14	1.407 (3)	C9—H9B	0.9700
C13—C18	1.412 (3)	O1—C7	1.233 (3)
C13—C12	1.454 (3)	C21—C22	1.363 (4)
C18—C17	1.414 (3)	C21—H21	0.9300
C18—C19	1.450 (3)	C7—C1	1.506 (4)
C19—C24	1.401 (3)	C23—C22	1.382 (4)
C19—C20	1.410 (3)	C23—H23	0.9300
C12—N2	1.414 (3)	C10—C11	1.508 (3)
N2—C10	1.461 (3)	C10—H10A	0.9700
N2—C9	1.477 (3)	C10—H10B	0.9700
C20—C21	1.412 (3)	C1—C6	1.380 (4)
C17—C16	1.375 (3)	C6—C5	1.376 (4)
C17—H17	0.9300	C6—H6	0.9300
C14—C15	1.372 (3)	C22—H22	0.9300
C14—H14	0.9300	C11—H11A	0.9700
C24—C23	1.370 (4)	C11—H11B	0.9700
C24—H24	0.9300	C4—C5	1.375 (5)
C15—C16	1.386 (3)	C4—H4	0.9300
C15—H15	0.9300	C5—H5	0.9300
N3—C7	1.347 (3)		

Table 4S: Bond Angles for **6b**

Atom—Atom—Atom	Angle/°	Atom—Atom—Atom	Angle/°
C3—C2—C1	120.3 (3)	N3—C8—H8B	109.6
C3—C2—H2	119.8	C9—C8—H8B	109.6
C1—C2—H2	119.8	H8A—C8—H8B	108.1
C4—C3—C2	119.6 (3)	N2—C9—C8	110.4 (2)
C4—C3—H3	120.2	N2—C9—H9A	109.6
C2—C3—H3	120.2	C8—C9—H9A	109.6
C12—N1—C20	118.5 (2)	N2—C9—H9B	109.6
C14—C13—C18	118.8 (2)	C8—C9—H9B	109.6
C14—C13—C12	123.0 (2)	H9A—C9—H9B	108.1
C18—C13—C12	118.1 (2)	C22—C21—C20	120.2 (2)
C13—C18—C17	118.6 (2)	C22—C21—H21	119.9
C13—C18—C19	118.5 (2)	C20—C21—H21	119.9
C17—C18—C19	122.8 (2)	O1—C7—N3	122.3 (2)
C24—C19—C20	118.6 (2)	O1—C7—C1	119.5 (2)
C24—C19—C18	123.8 (2)	N3—C7—C1	118.2 (2)
C20—C19—C18	117.6 (2)	C24—C23—C22	120.6 (2)
N1—C12—N2	117.88 (19)	C24—C23—H23	119.7
N1—C12—C13	123.8 (2)	C22—C23—H23	119.7
N2—C12—C13	118.2 (2)	N2—C10—C11	108.34 (19)
C12—N2—C10	116.41 (18)	N2—C10—H10A	110.0
C12—N2—C9	116.7 (2)	C11—C10—H10A	110.0
C10—N2—C9	108.16 (19)	N2—C10—H10B	110.0
N1—C20—C19	123.5 (2)	C11—C10—H10B	110.0
N1—C20—C21	117.2 (2)	H10A—C10—H10B	108.4
C19—C20—C21	119.3 (2)	C6—C1—C2	119.2 (3)
C16—C17—C18	121.0 (2)	C6—C1—C7	120.8 (2)
C16—C17—H17	119.5	C2—C1—C7	119.8 (3)
C18—C17—H17	119.5	C5—C6—C1	120.3 (3)

C15—C14—C13	121.0 (2)	C5—C6—H6	119.8
C15—C14—H14	119.5	C1—C6—H6	119.8
C13—C14—H14	119.5	C21—C22—C23	120.6 (3)
C23—C24—C19	120.7 (2)	C21—C22—H22	119.7
C23—C24—H24	119.6	C23—C22—H22	119.7
C19—C24—H24	119.7	N3—C11—C10	112.4 (2)
C14—C15—C16	120.4 (2)	N3—C11—H11A	109.1
C14—C15—H15	119.8	C10—C11—H11A	109.1
C16—C15—H15	119.8	N3—C11—H11B	109.1
C7—N3—C8	125.4 (2)	C10—C11—H11B	109.1
C7—N3—C11	119.9 (2)	H11A—C11—H11B	107.8
C8—N3—C11	114.63 (19)	C3—C4—C5	120.2 (3)
C17—C16—C15	120.0 (2)	C3—C4—H4	119.9
C17—C16—H16	120.0	C5—C4—H4	119.9
C15—C16—H16	120.0	C6—C5—C4	120.4 (3)
N3—C8—C9	110.40 (19)	C6—C5—H5	119.8
N3—C8—H8A	109.6	C4—C5—H5	119.8
C9—C8—H8A	109.6		

Table 5S: Dihedral angle for **6b**

Two planes	Angle/˚	Two planes	Angle/˚
C1—C2—C3—C4	−0.2 (5)	C18—C17—C16—C15	2.9 (5)
C14—C13—C18—C17	−2.9 (4)	C14—C15—C16—C17	−2.1 (5)
C12—C13—C18—C17	179.6 (2)	C7—N3—C8—C9	−135.9 (3)
C14—C13—C18—C19	176.5 (2)	C11—N3—C8—C9	47.5 (3)
C12—C13—C18—C19	−1.0 (4)	C12—N2—C9—C8	−161.6 (2)
C13—C18—C19—C24	−179.4 (2)	C10—N2—C9—C8	64.9 (3)
C17—C18—C19—C24	0.0 (4)	N3—C8—C9—N2	−55.3 (3)
C13—C18—C19—C20	1.7 (4)	N1—C20—C21—C22	179.3 (3)
C17—C18—C19—C20	−178.9 (2)	C19—C20—C21—C22	0.2 (4)
C20—N1—C12—N2	−175.7 (2)	C8—N3—C7—O1	168.8 (3)
C20—N1—C12—C13	0.2 (4)	C11—N3—C7—O1	−14.9 (4)
C14—C13—C12—N1	−177.4 (3)	C8—N3—C7—C1	−12.9 (4)
C18—C13—C12—N1	0.0 (4)	C11—N3—C7—C1	163.5 (3)
C14—C13—C12—N2	−1.5 (4)	C19—C24—C23—C22	0.1 (5)
C18—C13—C12—N2	175.9 (2)	C12—N2—C10—C11	162.6 (2)
N1—C12—N2—C10	16.8 (4)	C9—N2—C10—C11	−63.7 (3)
C13—C12—N2—C10	−159.3 (2)	C3—C2—C1—C6	−1.4 (4)
N1—C12—N2—C9	−112.9 (3)	C3—C2—C1—C7	−175.8 (3)
C13—C12—N2—C9	70.9 (3)	O1—C7—C1—C6	−55.1 (4)
C12—N1—C20—C19	0.6 (4)	N3—C7—C1—C6	126.5 (3)
C12—N1—C20—C21	−178.5 (3)	O1—C7—C1—C2	119.3 (3)
C24—C19—C20—N1	179.4 (2)	N3—C7—C1—C2	−59.1 (4)
C18—C19—C20—N1	−1.6 (4)	C2—C1—C6—C5	2.3 (4)
C24—C19—C20—C21	−1.5 (4)	C7—C1—C6—C5	176.7 (3)
C18—C19—C20—C21	177.4 (2)	C20—C21—C22—C23	1.3 (5)
C13—C18—C17—C16	−0.3 (4)	C24—C23—C22—C21	−1.5 (5)
C19—C18—C17—C16	−179.7 (3)	C7—N3—C11—C10	134.6 (3)
C18—C13—C14—C15	3.7 (4)	C8—N3—C11—C10	−48.7 (3)
C12—C13—C14—C15	−178.9 (3)	N2—C10—C11—N3	56.0 (3)
C20—C19—C24—C23	1.4 (4)	C2—C3—C4—C5	0.9 (5)
C18—C19—C24—C23	−177.5 (3)	C1—C6—C5—C4	−1.6 (5)
C13—C14—C15—C16	−1.2 (4)	C3—C4—C5—C6	0.0 (5)

Crystal data ***7d***

CHNOS
M_r = 459.60

Monoclinic, $P2_1/n$

a = 12.5058 (13) Å
b = 14.6774 (17) Å
c = 13.3524 (14) Å
β = 89.451 (9)°
V = 2450.8 (5) Å^3
Z = 4

$F(000)$ = 976.0
D_x = 1.246 Mg m^{-3}
Mo $K\alpha$ radiation, λ = 0.71073 Å
Cell parameters from 1760 reflections
θ = 3.2–29.2°
μ = 0.16 mm^{-1}
T = 293 K
, white
0.6 × 0.5 × 0.4 mm

Data collection

Radiation source: fine-focus sealed tube
Graphite monochromator
Absorption correction: multi-scan
?
T_{min} = 0.922, T_{max} = 1.000
7784 measured reflections
6663 independent reflections

3305 reflections with $I > 2\sigma(I)$
R_{int} = 0.018
θ_{max} = 29.2°, θ_{min} = 3.2°
h = −9→17
k = −16→20
l = −18→15

Refinement

Refinement on F^2
Least-squares matrix: full $R[F^2 > 2\sigma(F^2)]$ = 0.050
$wR(F^2)$ = 0.121
S = 1.02
5149 reflections
298 parameters
0 restraints
Primary atom site location: structure-invariant direct methods

Secondary atom site location: difference Fourier map Hydrogen site location: inferred from neighbouring sites
H atoms treated by a mixture of independent and constrained refinement
$w = 1/[\sigma^2(F_o^2) + (0.0438P)^2 + 0.1582P]$ where $P = (F_o^2 + 2F_c^2)/3$
$(\Delta/\sigma)_{max}$ = 0.001
$\Delta\rho_{max}$ = 0.14 e Å^{-3} $\Delta\rho_{min}$ = −0.25 e Å^{-3}

Table 6S: Fractional Atomic Coordinates ($\times 10^4$) and Equivalent Isotropic Displacement Parameters ($Å^2 \times 10^3$) for 6b. U_{eq} is defined as 1/3 of of the trace of the orthogonalised U_{IJ} tensor.

Atom	*x*	*y*	*z*	U_{iso}*/U_{eq}
S1	0.87179 (4)	0.19249 (4)	0.62715 (4)	0.05313 (17)
N2	0.90451 (12)	0.15341 (10)	0.29824 (11)	0.0437 (4)
O1	0.85352 (12)	0.28653 (10)	0.64877 (12)	0.0704 (5)
O2	0.95600 (10)	0.14456 (12)	0.67589 (11)	0.0700 (5)
N3	1.02859 (12)	0.10726 (10)	0.17912 (11)	0.0440 (4)
N1	0.89739 (12)	0.18566 (10)	0.50721 (11)	0.0444 (4)
C16	0.86887 (14)	0.18206 (13)	0.11995 (15)	0.0445 (5)
C8	0.75352 (14)	0.13109 (14)	0.64929 (14)	0.0465 (5)
C22	1.00718 (15)	0.13476 (13)	−0.00057 (14)	0.0462 (5)
C15	0.93860 (14)	0.14755 (12)	0.19725 (13)	0.0392 (4)
C21	0.90525 (15)	0.17769 (13)	0.01987 (15)	0.0482 (5)
C14	0.89796 (16)	0.24619 (13)	0.33966 (15)	0.0508 (5)
H14A	0.8606	0.2855	0.2933	0.061*
H14B	0.9694	0.2703	0.3486	0.061*
C23	1.06275 (14)	0.09828 (13)	0.08049 (14)	0.0441 (5)
C12	0.96299 (15)	0.09523 (14)	0.36699 (14)	0.0508 (5)
H12A	1.0351	0.1184	0.3749	0.061*
H12B	0.9677	0.0340	0.3399	0.061*
C13	0.83968 (16)	0.24495 (13)	0.43846 (15)	0.0504 (5)
H13A	0.8356	0.3062	0.4657	0.060*
H13B	0.7674	0.2225	0.4295	0.060*
C27	1.05135 (18)	0.12372 (16)	−0.09680 (16)	0.0622 (6)
H27	1.0162	0.1480	−0.1517	0.075*
C11	0.90694 (16)	0.09288 (13)	0.46703 (14)	0.0513 (5)
H11A	0.8364	0.0664	0.4597	0.062*
H11B	0.9470	0.0553	0.5131	0.062*
C5	0.56493 (15)	0.03232 (14)	0.67638 (15)	0.0490 (5)
C24	1.15876 (15)	0.05188 (14)	0.06368 (17)	0.0558 (5)
H24	1.1959	0.0279	0.1176	0.067*
C9	0.65609 (16)	0.17097 (15)	0.62998 (16)	0.0556 (6)
H9	0.6528	0.2311	0.6082	0.067*
C25	1.19867 (18)	0.04137 (16)	−0.03106 (18)	0.0656 (6)
H25	1.2621	0.0095	−0.0415	0.079*
C6	0.66410 (16)	−0.00622 (15)	0.69497 (17)	0.0596 (6)
H6	0.6676	−0.0662	0.7171	0.072*
C20	0.83837 (19)	0.20989 (17)	−0.05630 (18)	0.0695 (7)
H20	0.8620	0.2082	−0.1225	0.083*
C2	0.46293 (16)	−0.02121 (15)	0.69611 (18)	0.0589 (6)
C10	0.56375 (16)	0.12128 (14)	0.64320 (16)	0.0562 (6)
H10	0.4984	0.1486	0.6293	0.067*
C7	0.75710 (16)	0.04200 (15)	0.68149 (16)	0.0577 (6)
H7	0.8226	0.0145	0.6941	0.069*
C3	0.36522 (16)	0.02238 (18)	0.6496 (2)	0.0959 (10)
H3A	0.3746	0.0253	0.5782	0.144*
H3B	0.3562	0.0828	0.6758	0.144*
H3C	0.3030	−0.0134	0.6654	0.144*
C17	0.76540 (16)	0.21474 (15)	0.13892 (18)	0.0602 (6)
H17	0.7392	0.2157	0.2043	0.072*

C26	1.1454 (2)	0.07774 (17)	−0.11104 (18)	0.0702 (7)
H26	1.1734	0.0711	−0.1754	0.084*
C4	0.47333 (19)	−0.11869 (16)	0.6557 (2)	0.0801 (8)
H4A	0.5347	−0.1474	0.6845	0.120*
H4B	0.4815	−0.1169	0.5841	0.120*
H4C	0.4103	−0.1527	0.6730	0.120*
C18	0.70249 (19)	0.24507 (19)	0.0633 (2)	0.0832 (8)
H18	0.6342	0.2670	0.0773	0.100*
C1	0.4469 (2)	−0.02644 (18)	0.80942 (19)	0.0864 (8)
H1A	0.5084	−0.0543	0.8392	0.130*
H1B	0.3845	−0.0622	0.8244	0.130*
H1C	0.4377	0.0339	0.8359	0.130*
C19	0.7404 (2)	0.2432 (2)	−0.0348 (2)	0.0903 (9)
H19	0.6977	0.2652	−0.0861	0.108*

Table 7S: Anisotropic Displacement Parameters ($Å^2 \times 10^3$) for 6a. The Anisotropic displacement factor exponent takes the form: $-2\pi^2[h^2a^{*2}U_{11}+...+2hka\times b\times U_{12}]$

Atom	U^{11}	U^{22}	U^{33}	U^{12}	U^{13}	U^{23}
S1	0.0594 (3)	0.0670 (4)	0.0330 (3)	−0.0039(3)	−0.001(2)	−0.0050(2)
N2	0.0618 (9)	0.0366 (9)	0.0327 (9)	0.0049(7)	0.0026(7)	0.0039(7)
O1	0.0942 (11)	0.0632 (11)	0.0538 (10)	−0.0137(8)	0.0063(9)	−0.0220(8)
O2	0.0588 (8)	0.1098 (14)	0.0418 (9)	−0.0016(8)	0.0125(7)	0.0081(8)
N3	0.0528 (9)	0.0446 (10)	0.0345 (9)	−0.004(7)	0.0011(7)	0.0013(7)
N1	0.0562 (9)	0.0451 (10)	0.0319 (9)	0.0048(7)	0.0012(7)	0.0021(7)
C16	0.0489 (10)	0.0431 (12)	0.0416 (12)	−0.0099(9)	−0.0041(9)	0.0053(9)
C8	0.0546 (11)	0.0520 (13)	0.0329 (11)	0.0074(9)	0.0047(9)	0.0016(9)
C22	0.0582 (11)	0.0482 (12)	0.0320 (11)	−0.0205(9)	0.0004(9)	−0.0002(9)
C15	0.0500 (10)	0.0361 (10)	0.0316 (10)	−0.0055(8)	0.0016(8)	0.0026(8)
C21	0.0580 (11)	0.0487 (12)	0.0381 (12)	−0.0171(9)	−0.0081(9)	0.0070(7)
C14	0.0724 (12)	0.0403 (12)	0.0395 (12)	0.0046(10)	0.0041(10)	0.0063(7)
C23	0.0550 (11)	0.0421 (11)	0.0351 (11)	−0.0130(9)	0.0042(9)	−0.0030(9)
C12	0.0695 (12)	0.0477 (12)	0.0352 (11)	0.0157(10)	0.0039(9)	0.0069(9)
C13	0.0675 (12)	0.0423 (12)	0.0414 (12)	0.0107(10)	0.0020(10)	0.0013(9)
C27	0.0780 (15)	0.0738 (16)	0.0346 (12)	−0.0287(12)	−0.0012(11)	−0.0012(11)
C11	0.0722 (12)	0.0458 (12)	0.0358 (11)	0.0139(10)	0.0047(10)	0.0089(9)
C5	0.0563 (11)	0.0497 (13)	0.0408 (12)	0.0075(10)	0.0065(9)	−0.0009(9)
C24	0.0585 (12)	0.0577 (14)	0.0511 (14)	−0.0055(10)	0.0072(10)	−0.0018(11)
C9	0.0614 (12)	0.0464 (13)	0.0590 (14)	0.0131(10)	0.0098(11)	0.0040(10)
C25	0.0682 (13)	0.0660 (16)	0.0621 (16)	−0.0139(12)	0.0223(12)	−0.0115(13)
C6	0.0591 (12)	0.0527 (13)	0.0669 (16)	0.0101(11)	0.0069(11)	0.0179(11)
C20	0.0728 (15)	0.0898 (19)	0.0462 (14)	−0.0140(13)	−0.0148(12)	0.0196(12)
C2	0.0579 (12)	0.0540 (14)	0.0647 (16)	0.0018(10)	0.0112(11)	−0.0081(11)
C10	0.0523 (11)	0.0527 (13)	0.0635 (15)	0.0154(10)	0.0085(10)	0.0024(11)
C7	0.0545 (12)	0.0650 (15)	0.0536 (14)	0.0154(11)	0.0028(10)	0.0164(11)
C3	0.0566 (14)	0.084 (2)	0.147 (3)	−0.0009(13)	−0.0066(16)	0.0004(18)
C17	0.0557 (12)	0.0663 (16)	0.0586 (15)	−0.0017(10)	−0.0005(11)	0.0094(11)
C26	0.0816 (16)	0.0805 (18)	0.0479 (15)	−0.0313(14)	0.0240(13)	−0.0143(13)
C4	0.0890 (16)	0.0647 (17)	0.086 (2)	−0.0047(13)	0.0095(15)	−0.0176(14)
C18	0.0584 (14)	0.100(2)	0.091 (2)	0.0077(13)	−0.0093 (14)	0.0243(17)
C1	0.0956 (17)	0.08(2)	0.0754 (19)	−0.0198(15)	0.0381(15)	−0.0135(15)
C19	0.0772 (17)	0.120(3)	0.074 (2)	−0.0002 (16)	−0.0238 (15)	0.0337(18)

Table 8S: Bond Lengths for **7d**

Atom—Atom	Length/Å	Atom—Atom	Length/Å
S1—O2	1.4286 (15)	C5—C6	1.388 (3)
S1—N1	1.6332 (16)	C5—C2	1.519 (3)
S1—C8	1.7546 (19)	C24—C25	1.364 (3)
N2—C15	1.413 (2)	C24—H24	0.9300
N2—C12	1.456 (2)	C9—C10	1.376 (3)
N2—C14	1.472 (2)	C9—H9	0.9300
N3—C15	1.292 (2)	C25—C26	1.373 (3)
N3—C23	1.387 (2)	C25—H25	0.9300
N1—C13	1.461 (2)	C6—C7	1.372 (3)
N1—C11	1.468 (2)	C6—H6	0.9300
C16—C17	1.401 (3)	C20—C19	1.348 (3)
C16—C21	1.409 (3)	C20—H20	0.9300
C16—C15	1.449 (3)	C2—C3	1.517 (3)
C8—C7	1.377 (3)	C2—C1	1.526 (3)
C8—C9	1.378 (3)	C2—C4	1.534 (3)
C22—C23	1.398 (3)	C10—H10	0.9300
C22—C27	1.403 (3)	C7—H7	0.9300
C22—C21	1.446 (3)	C3—H3A	0.9600
C21—C20	1.405 (3)	C3—H3B	0.9600
C14—C13	1.501 (2)	C3—H3C	0.9600
C14—H14A	0.9700	C17—C18	1.361 (3)
C14—H14B	0.9700	C17—H17	0.9300
C23—C24	1.397 (3)	C26—H26	0.9300
C12—C11	1.503 (2)	C4—H4A	0.9600
C12—H12A	0.9700	C4—H4B	0.9600
C12—H12B	0.9700	C4—H4C	0.9600
C13—H13A	0.9700	C18—C19	1.389 (4)
C13—H13B	0.9700	C18—H18	0.9300
C27—C26	1.367 (3)	C1—H1A	0.9600
C27—H27	0.9300	C1—H1B	0.9600
C11—H11A	0.9700	C1—H1C	0.9600
C11—H11B	0.9700	C19—H19	0.9300

Table 9S: Bond Angles for **7d**

Atom—Atom—Atom	Angle/˚	Atom—Atom—Atom	Angle/˚
O1—S1—O2	120.07 (10)	C10—C5—C2	122.27 (18)
O1—S1—N1	106.69 (9)	C6—C5—C2	120.57 (19)
O2—S1—N1	106.14 (8)	C25—C24—C23	120.7 (2)
O1—S1—C8	109.23 (9)	C25—C24—H24	119.7
O2—S1—C8	107.11 (9)	C23—C24—H24	119.7
N1—S1—C8	106.90 (9)	C10—C9—C8	119.6 (2)
C15—N2—C12	114.66 (14)	C10—C9—H9	120.2
C15—N2—C14	115.48 (14)	C8—C9—H9	120.2
C12—N2—C14	109.40 (15)	C24—C25—C26	120.1 (2)
C15—N3—C23	118.76 (17)	C24—C25—H25	120.0
C13—N1—C11	111.22 (15)	C26—C25—H25	120.0
C13—N1—S1	119.09 (12)	C7—C6—C5	121.6 (2)
C11—N1—S1	115.46 (12)	C7—C6—H6	119.2
C17—C16—C21	118.45 (19)	C5—C6—H6	119.2

C17—C16—C15	123.51 (19)	C19—C20—C21	120.9 (2)
C21—C16—C15	117.95 (17)	C19—C20—H20	119.5
C7—C8—C9	119.54 (18)	C21—C20—H20	119.5
C7—C8—S1	120.69 (15)	C3—C2—C5	112.90 (19)
C9—C8—S1	119.71 (16)	C3—C2—C1	109.17 (19)
C23—C22—C27	118.05 (19)	C5—C2—C1	107.45 (19)
C23—C22—C21	117.69 (17)	C3—C2—C4	108.4 (2)
C27—C22—C21	124.2 (2)	C5—C2—C4	110.67 (17)
N3—C15—N2	117.45 (16)	C1—C2—C4	108.18 (19)
N3—C15—C16	123.75 (17)	C9—C10—C5	122.12 (18)
N2—C15—C16	118.71 (16)	C9—C10—H10	118.9
C20—C21—C16	118.8 (2)	C5—C10—H10	118.9
C20—C21—C22	122.7 (2)	C6—C7—C8	120.05 (18)
C16—C21—C22	118.36 (18)	C6—C7—H7	120.0
N2—C14—C13	110.11 (15)	C8—C7—H7	120.0
N2—C14—H14A	109.6	C2—C3—H3A	109.5
C13—C14—H14A	109.6	C2—C3—H3B	109.5
N2—C14—H14B	109.6	H3A—C3—H3B	109.5
C13—C14—H14B	109.6	C2—C3—H3C	109.5
H14A—C14—H14B	108.2	H3A—C3—H3C	109.5
N3—C23—C24	117.09 (18)	H3B—C3—H3C	109.5
N3—C23—C22	123.21 (17)	C18—C17—C16	121.2 (2)
C24—C23—C22	119.68 (18)	C18—C17—H17	119.4
N2—C12—C11	109.94 (14)	C16—C17—H17	119.4
N2—C12—H12A	109.7	C27—C26—C25	120.5 (2)
C11—C12—H12A	109.7	C27—C26—H26	119.8
N2—C12—H12B	109.7	C25—C26—H26	119.8
C11—C12—H12B	109.7	C2—C4—H4A	109.5
H12A—C12—H12B	108.2	C2—C4—H4B	109.5
N1—C13—C14	108.71 (15)	H4A—C4—H4B	109.5
N1—C13—H13A	109.9	C2—C4—H4C	109.5
C14—C13—H13A	109.9	H4A—C4—H4C	109.5
N1—C13—H13B	109.9	H4B—C4—H4C	109.5
C14—C13—H13B	109.9	C17—C18—C19	119.9 (2)
H13A—C13—H13B	108.3	C17—C18—H18	120.0
C26—C27—C22	121.0 (2)	C19—C18—H18	120.0
C26—C27—H27	119.5	C2—C1—H1A	109.5
C22—C27—H27	119.5	C2—C1—H1B	109.5
N1—C11—C12	109.83 (15)	H1A—C1—H1B	109.5
N1—C11—H11A	109.7	C2—C1—H1C	109.5
C12—C11—H11A	109.7	H1A—C1—H1C	109.5
N1—C11—H11B	109.7	H1B—C1—H1C	109.5
C12—C11—H11B	109.7	C20—C19—C18	120.6 (2)
H11A—C11—H11B	108.2	C20—C19—H19	119.7
C10—C5—C6	117.11 (18)	C18—C19—H19	119.7

Table 10S: Dihedral angle for **7d**

Two planes	Angle/˚	Two planes	Angle/˚
O1—S1—N1—C13	−37.12 (16)	C15—N2—C12—C11	−168.92 (16)
O2—S1—N1—C13	−166.26 (15)	C14—N2—C12—C11	59.5 (2)
C8—S1—N1—C13	79.65(16)	C11—N1—C13—C14	−58.4 (2)
O1—S1—N1—C11	−173.48 (14)	S1—N1—C13—C14	163.59 (13)

O2—S1—N1—C11	57.38(16)	N2—C14—C13—N1	59.5 (2)
C8—S1—N1—C11	−56.70 (15)	C23—C22—C27—C26	0.7 (3)
O1—S1—C8—C7	−148.45 (17)	C21—C22—C27—C26	−176.19 (19)
O2—S1—C8—C7	−17.0 (2)	C13—N1—C11—C12	57.9 (2)
N1—S1—C8—C7	96.47 (18)	S1—N1—C11—C12	−162.41 (13)
O1—S1—C8—C9	34.50 (19)	N2—C12—C11—N1	−58.0 (2)
O2—S1—C8—C9	166.00 (16)	N3—C23—C24—C25	−178.98 (18)
N1—S1—C8—C9	−80.58 (18)	C22—C23—C24—C25	−0.3 (3)
C23—N3—C15—N2	178.28 (15)	C7—C8—C9—C10	0.0 (3)
C23—N3—C15—C16	1.8 (3)	S1—C8—C9—C10	177.13 (16)
C12—N2—C15—N3	−13.4 (2)	C23—C24—C25—C26	1.0 (3)
C14—N2—C15—N3	115.17 (18)	C10—C5—C6—C7	0.3 (3)
C12—N2—C15—C16	163.22 (16)	C2—C5—C6—C7	−177.4 (2)
C14—N2—C15—C16	−68.2 (2)	C16—C21—C20—C19	−1.0 (3)
C17—C16—C15—N3	171.27 (18)	C22—C21—C20—C19	174.9 (2)
C21—C16—C15—N3	−5.1 (3)	C10—C5—C2—C3	15.8 (3)
C17—C16—C15—N2	−5.1 (3)	C6—C5—C2—C3	−166.7 (2)
C21—C16—C15—N2	178.48 (16)	C10—C5—C2—C1	−104.7 (2)
C17—C16—C21—C20	2.8 (3)	C6—C5—C2—C1	72.9 (2)
C15—C16—C21—C20	179.32 (18)	C10—C5—C2—C4	137.4 (2)
C17—C16—C21—C22	−173.31 (17)	C6—C5—C2—C4	−45.0 (3)
C15—C16—C21—C22	3.3 (3)	C8—C9—C10—C5	0.7 (3)
C23—C22—C21—C20	−174.58 (18)	C6—C5—C10—C9	−0.8 (3)
C27—C22—C21—C20	2.3 (3)	C2—C5—C10—C9	176.8 (2)
C23—C22—C21—C16	1.3 (3)	C5—C6—C7—C8	0.4 (4)
C27—C22—C21—C16	178.24 (18)	C9—C8—C7—C6	−0.6 (3)
C15—N2—C14—C13	168.12 (16)	S1—C8—C7—C6	−177.61 (17)
C12—N2—C14—C13	−60.7 (2)	C21—C16—C17—C18	−2.6 (3)
C15—N3—C23—C24	−178.08 (17)	C15—C16—C17—C18	−178.9 (2)
C15—N3—C23—C22	3.3 (3)	C22—C27—C26—C25	−0.1 (3)
C27—C22—C23—N3	178.04 (17)	C24—C25—C26—C27	−0.8 (3)
C21—C22—C23—N3	−4.8 (3)	C16—C17—C18—C19	0.5 (4)
C27—C22—C23—C24	−0.5 (3)	C21—C20—C19—C18	−1.1 (4)
C21—C22—C23—C24	176.59 (17)	C17—C18—C19—C20	1.4 (4)